US 20250266808A1

(19) **United States**

(12) **Patent Application Publication** (10) **Pub. No.: US 2025/0266808 A1**

MCHUGH et al. (43) **Pub. Date: Aug. 21, 2025**

(54) **ACOUSTIC RESONATOR WITH ASPECT RATIO FOR SPUR REDUCTION**

(71) Applicant: **Murata Manufacturing Co., Ltd.**, Nagaokakyo-shi (JP)

(72) Inventors: **Sean MCHUGH**, Santa Barbara, CA (US); **Julius KOSKELA**, Helsinki (FI); **Soumya YANDRAPALLI**, Amsterdam (NL); **Drew MOROSIN**, Oxnard, CA (US)

(21) Appl. No.: **19/025,547**

(22) Filed: **Jan. 16, 2025**

Related U.S. Application Data

(60) Provisional application No. 63/623,117, filed on Jan. 19, 2024.

Publication Classification

(51) **Int. Cl.**

H03H 9/17	(2006.01)
H03H 9/02	(2006.01)
H03H 9/13	(2006.01)
H03H 9/56	(2006.01)

(52) **U.S. Cl.**

CPC ***H03H 9/174*** (2013.01); ***H03H 9/02133*** (2013.01); ***H03H 9/131*** (2013.01); ***H03H 9/568*** (2013.01)

(57) **ABSTRACT**

An acoustic resonator is provided that includes nanowires that each include a piezoelectric layer having first and second surfaces; a first electrode on the first surface; and a second electrode on the second surface. The nanowires each extend from a first busbar predominantly in a first direction, such that a space is defined between a pair of nanowires of the plurality of nanowires in a second direction that is substantially perpendicular to the first direction, such that there is no piezoelectric material between the pair of nanowires in the second direction. The nanowires each comprise a height in a thickness direction that is substantially orthogonal to the first and second directions. The nanowires each comprises a ratio of a width in the second direction of at least one of the first electrode and the second electrode to the height of the nanowire that is less than 2.

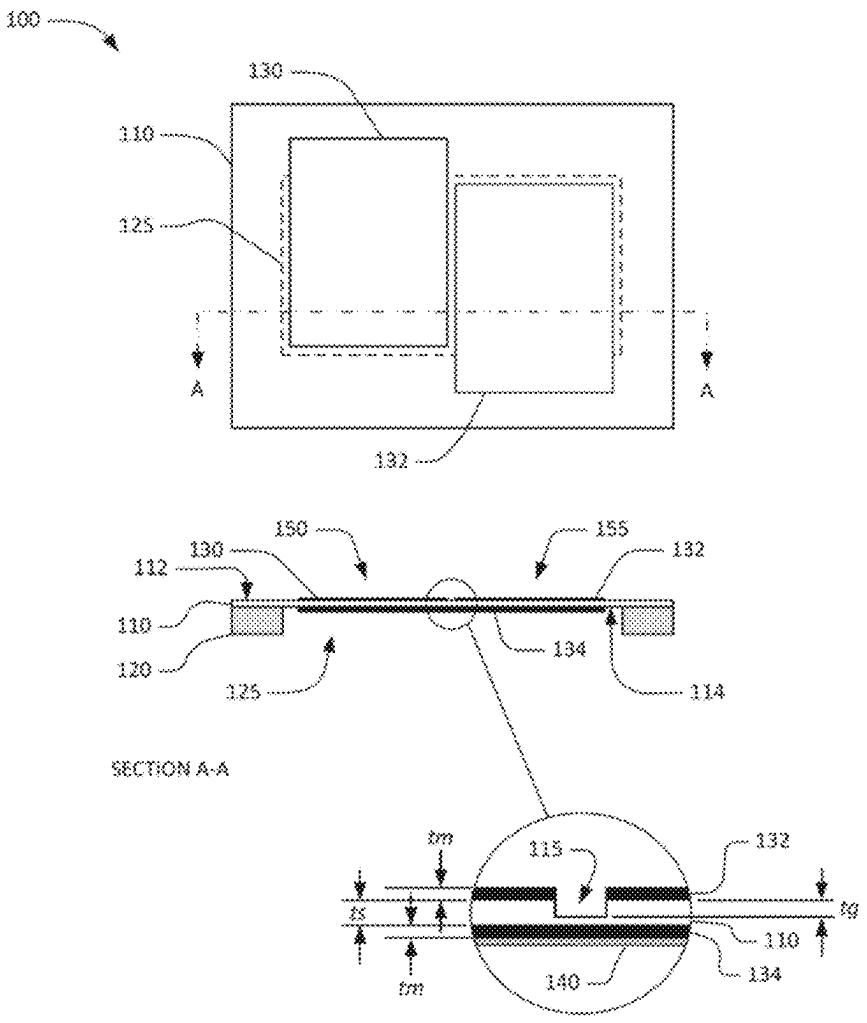

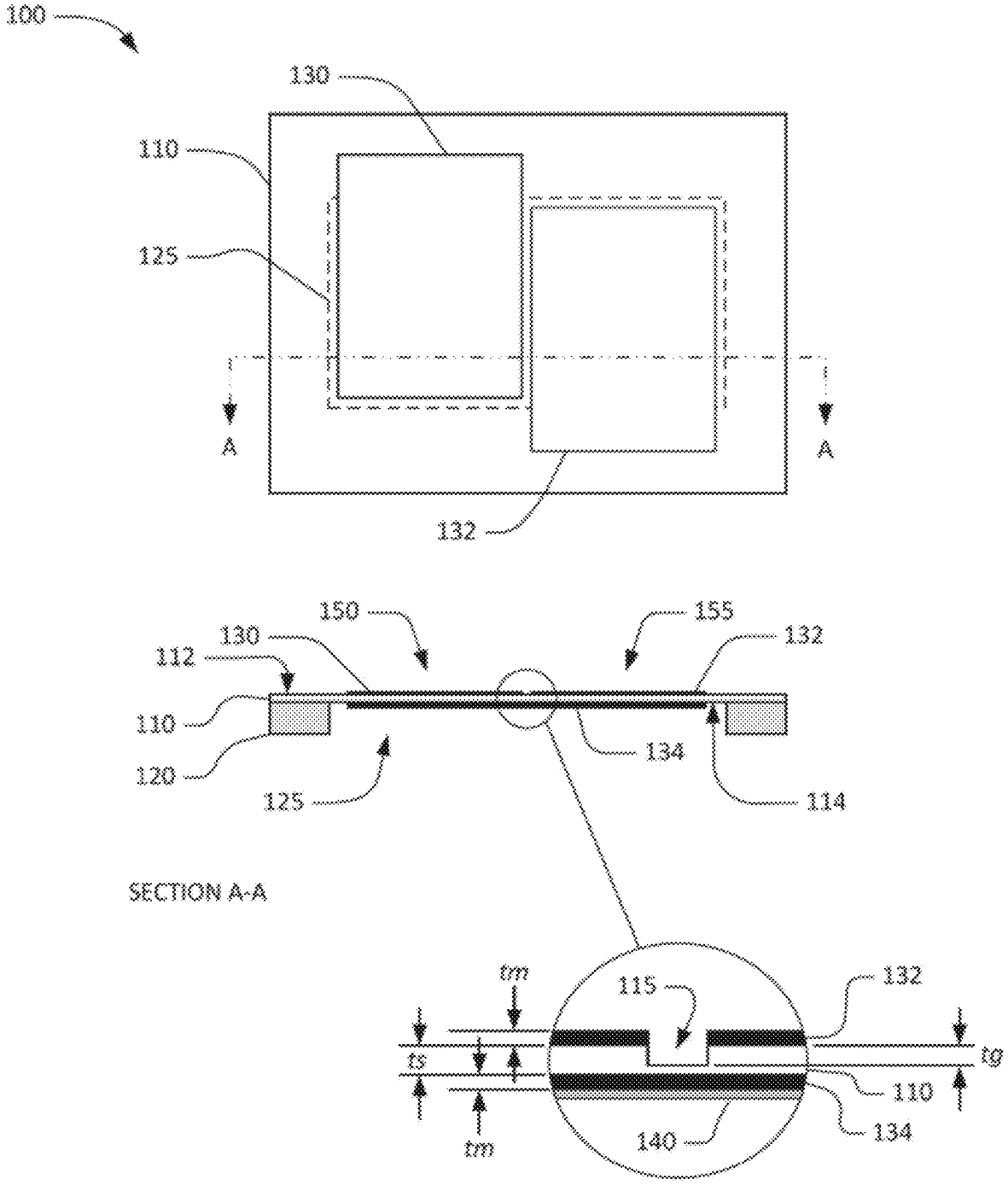
100
130
110
125
A
A
132
150
155
130
132
112
110
120
125
134
114
SECTION A-A
tm
115
132
ts
tg
110
134
140
tm

FIG. 1

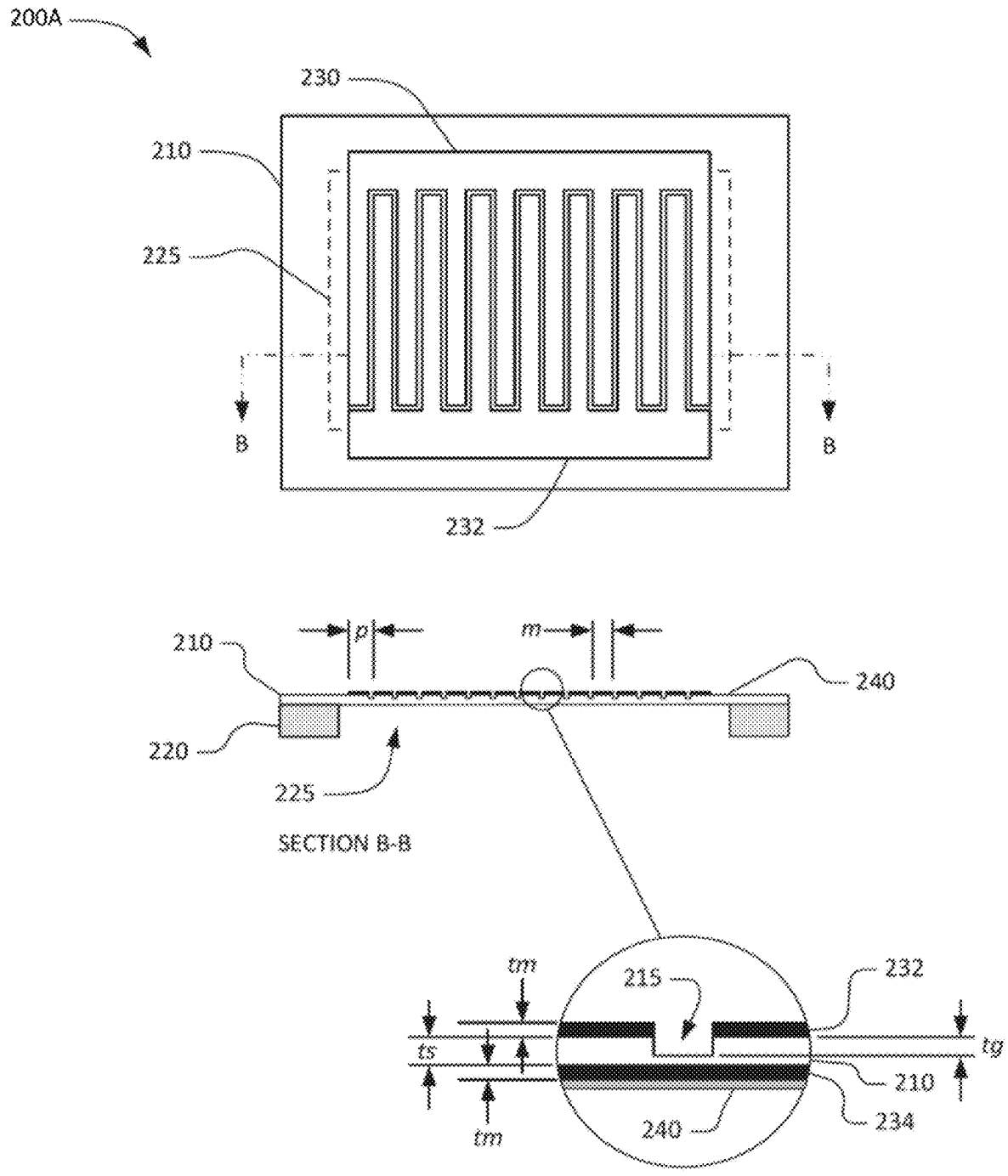
200A
230
210
225
B
B
232
210
p
m
240
220
225
SECTION B-B
tm
215
232
ts
tg
210
240
234
tm

FIG. 2A

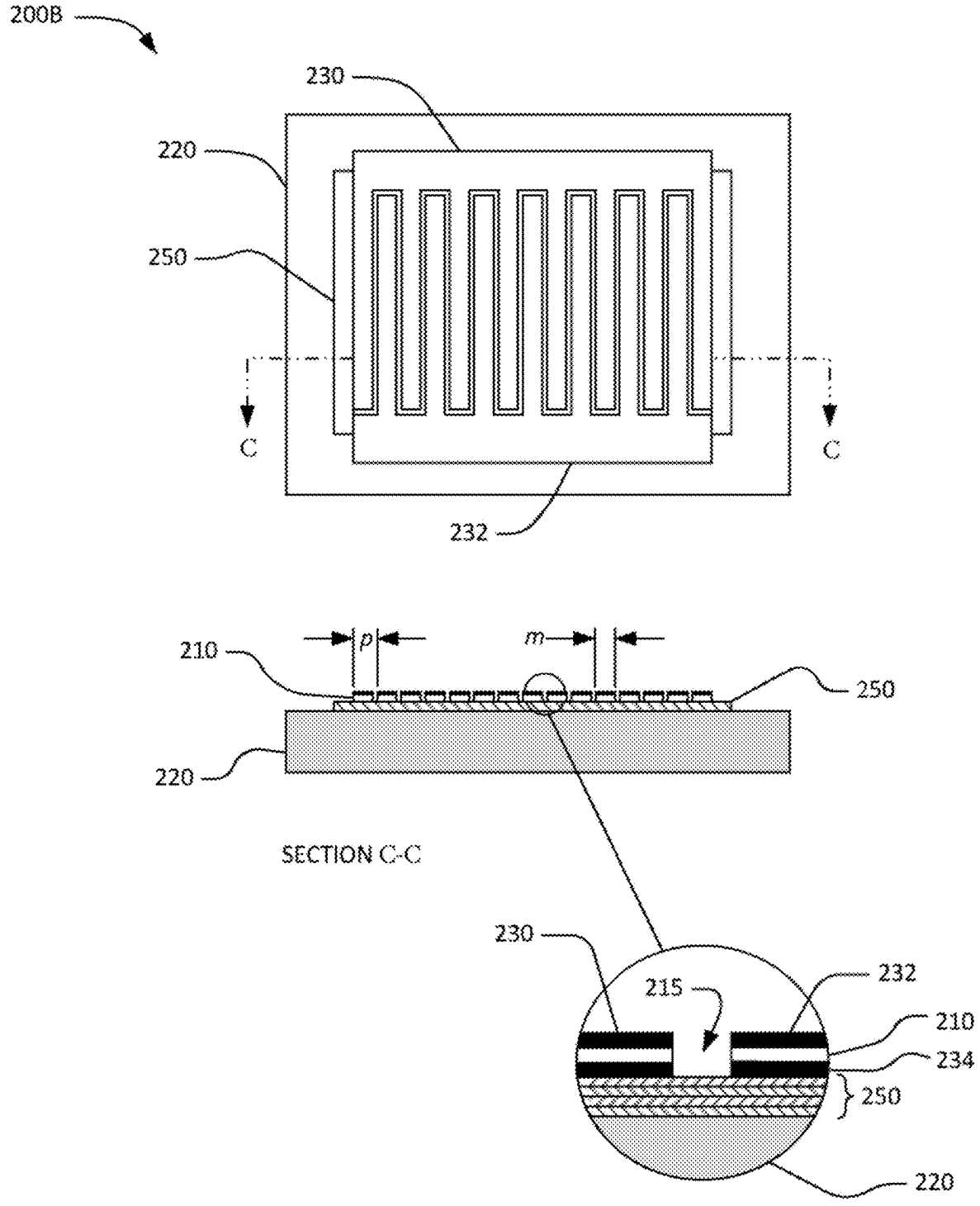
200B
230
220
250
C
C
232
210
p
m
250
220
SECTION C-C
230
215
232
210
234
250
220

FIG. 2B

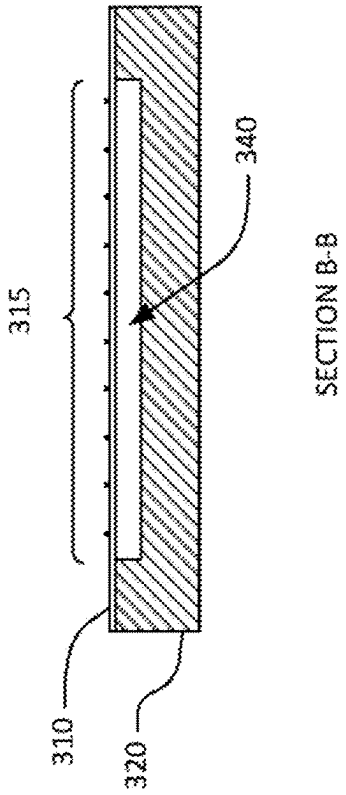

FIG. 3A

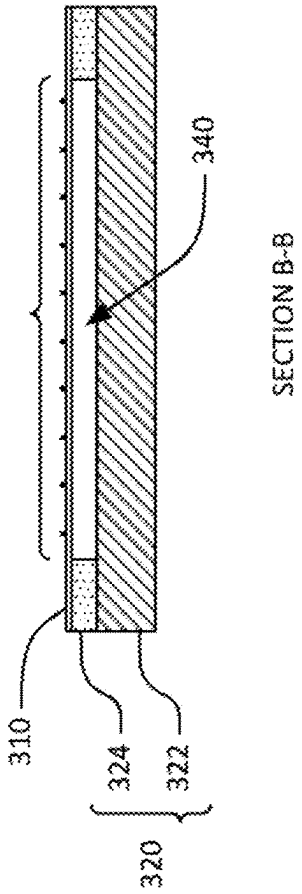

FIG. 3B

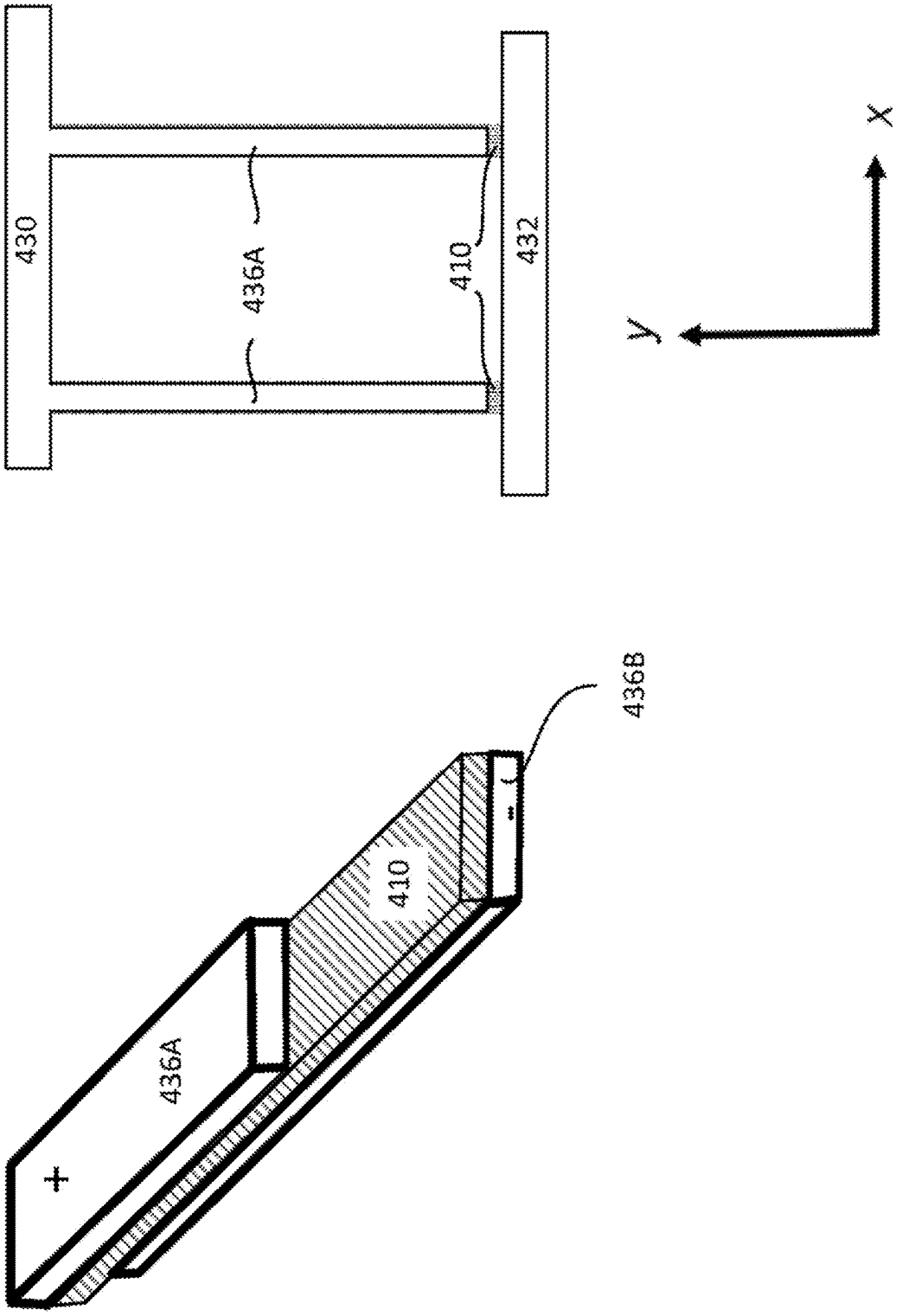

FIG. 4A

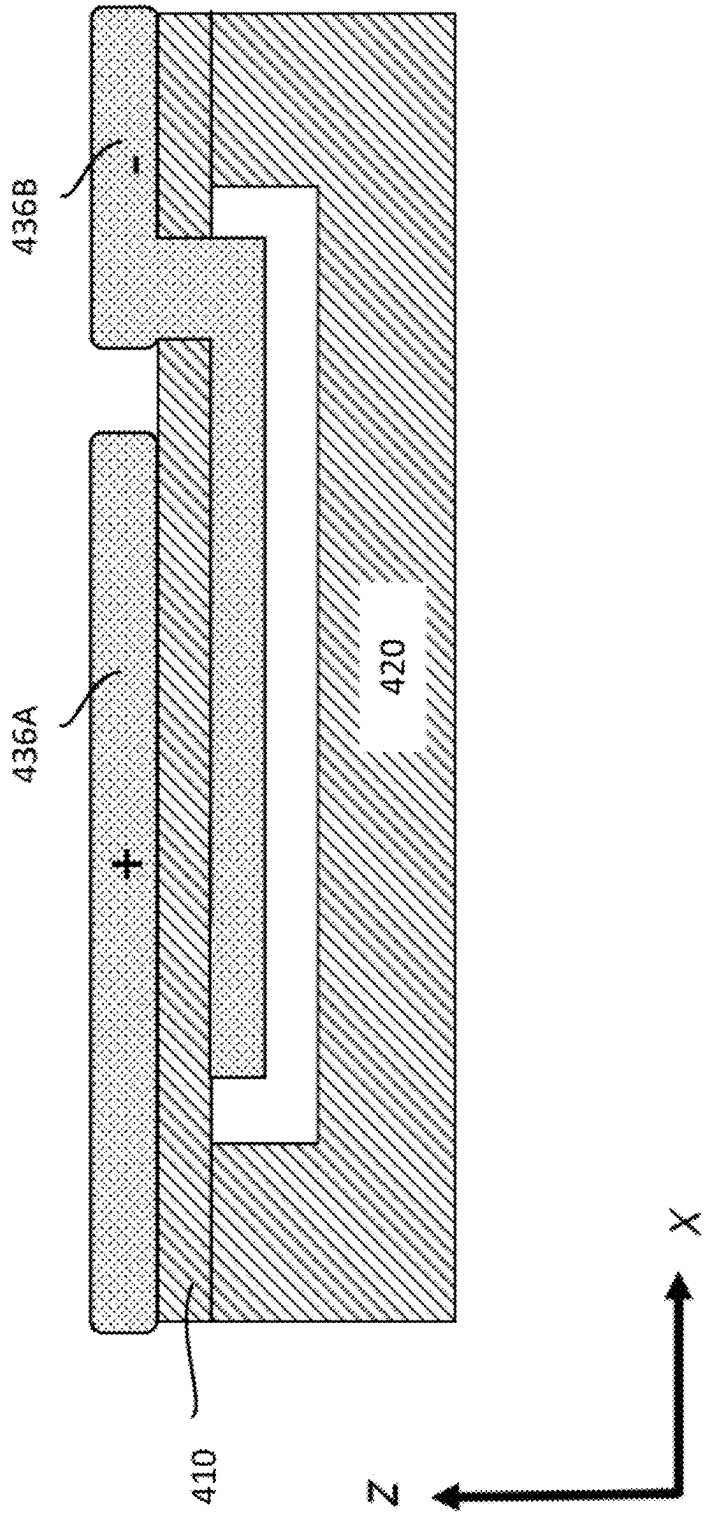

FIG. 4B

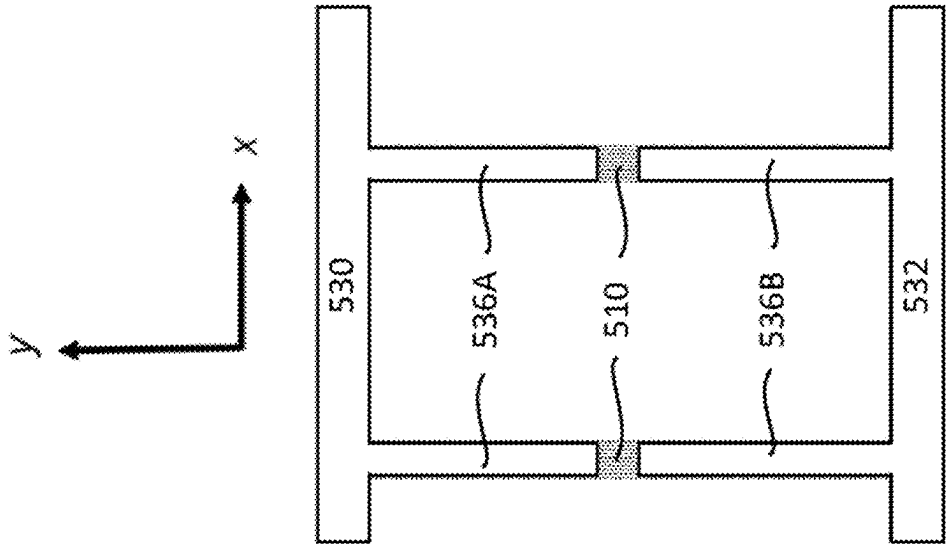

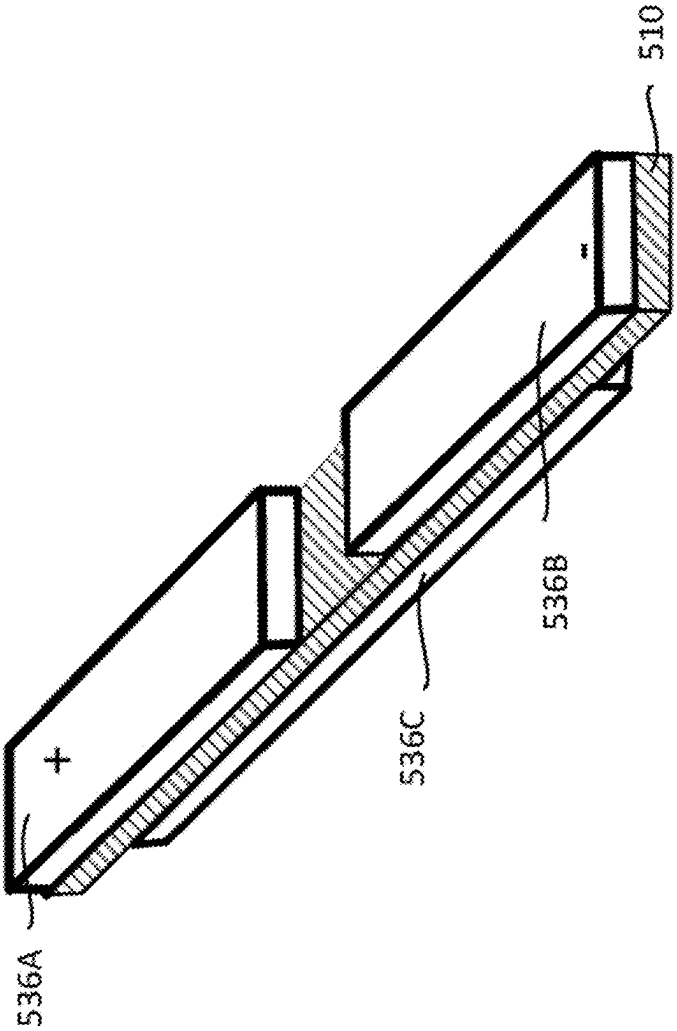

FIG. 5

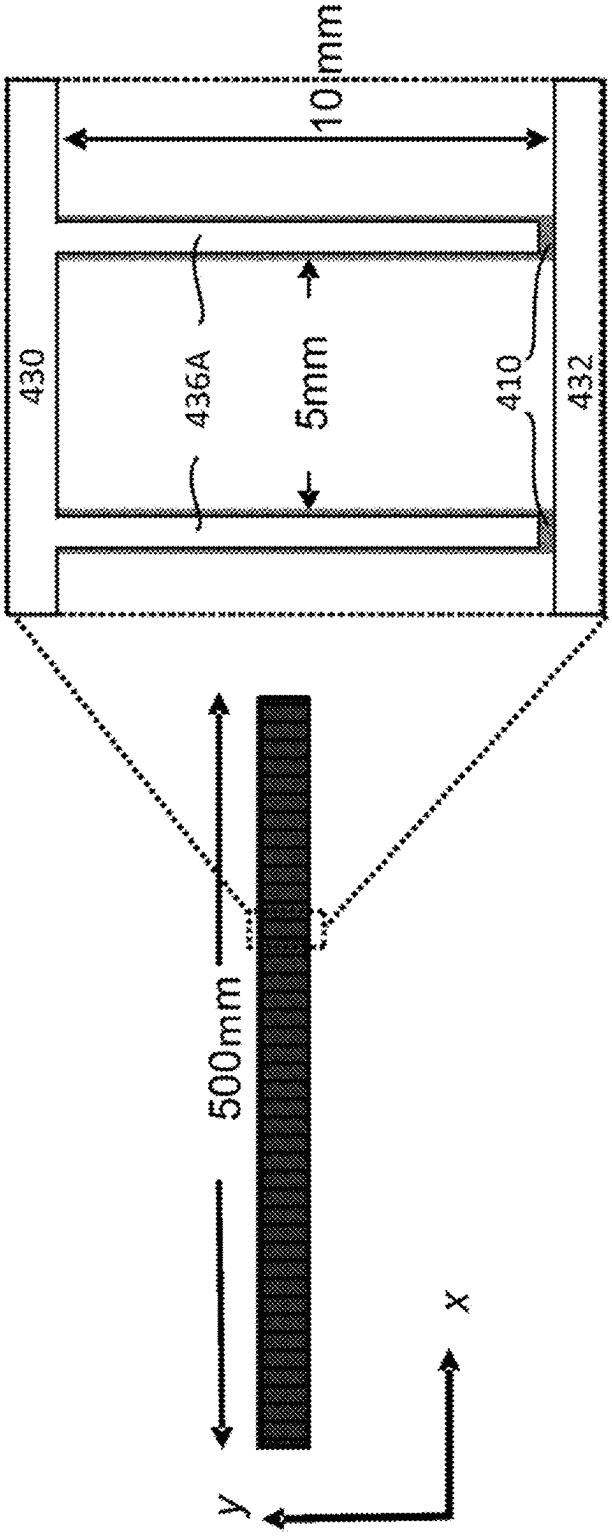

FIG. 6

FIG. 7A

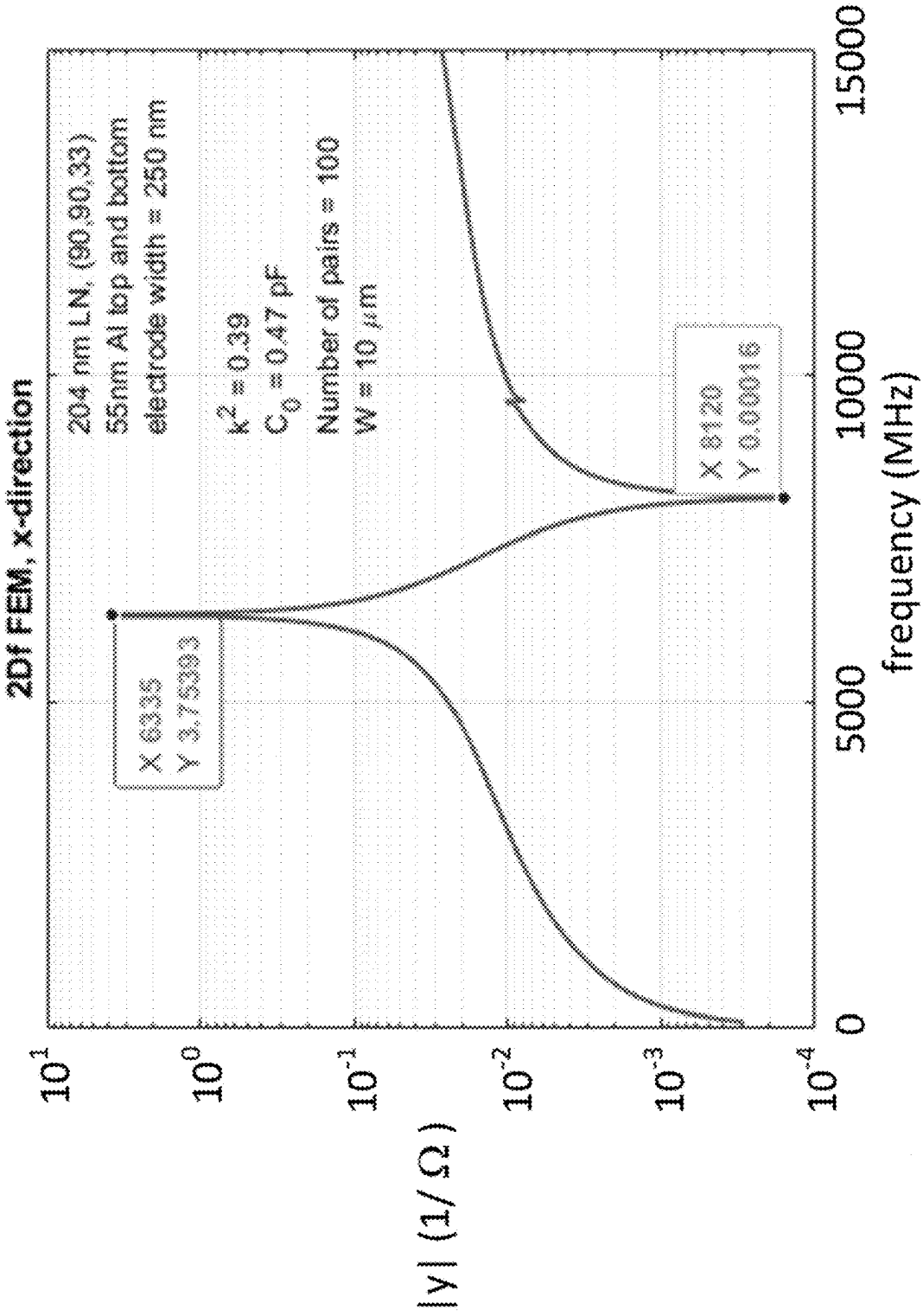
2Df FEM, x-direction
204 nm LN, (90,90,33)
55nm Al top and bottom
electrode width = 250 nm
k^2 = 0.39
C_0 = 0.47 pF
Number of pairs = 100
W = 10 μm
X 6335
Y 3.75283
X 8120
Y 0.00016
|Y| (1/ Ω)
frequency (MHz)
10^{-1}
10^{0}
10^{-1}
10^{-2}
10^{-3}
10^{-4}
0
5000
10000
15000

FIG. 7B

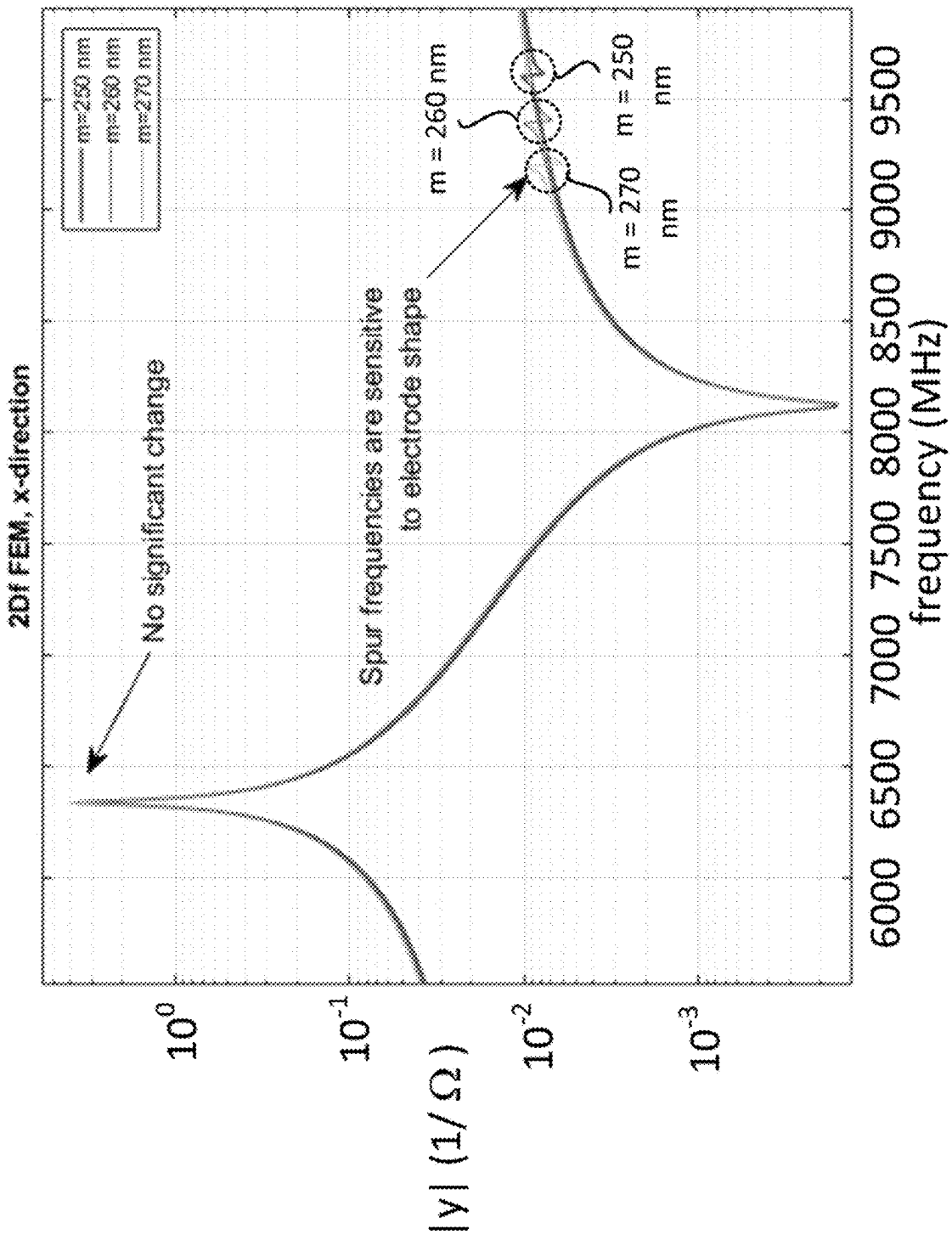
2Df FEM, x-direction
m=250 nm
m=260 nm
m=270 nm
No significant change
Spur frequencies are sensitive
to electrode shape
m = 260 nm
m = 270 nm
m = 250 nm
|y| (1/Ω)
10^0
10^-1
10^-2
10^-3
6000 6500 7000 7500 8000 8500 9000 9500
frequency (MHz)

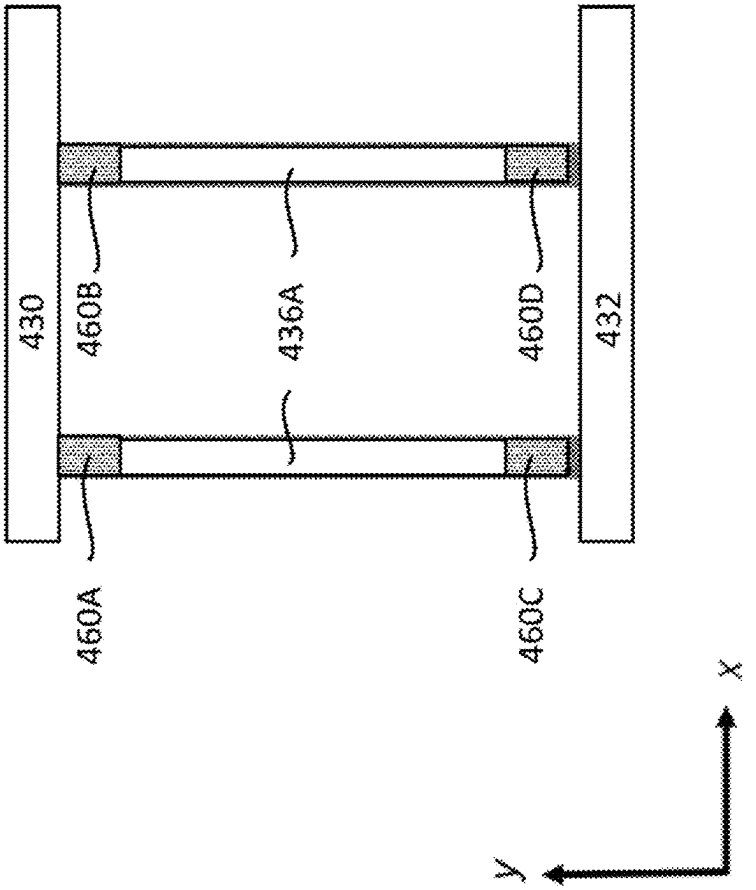

FIG. 8

FIG. 9A

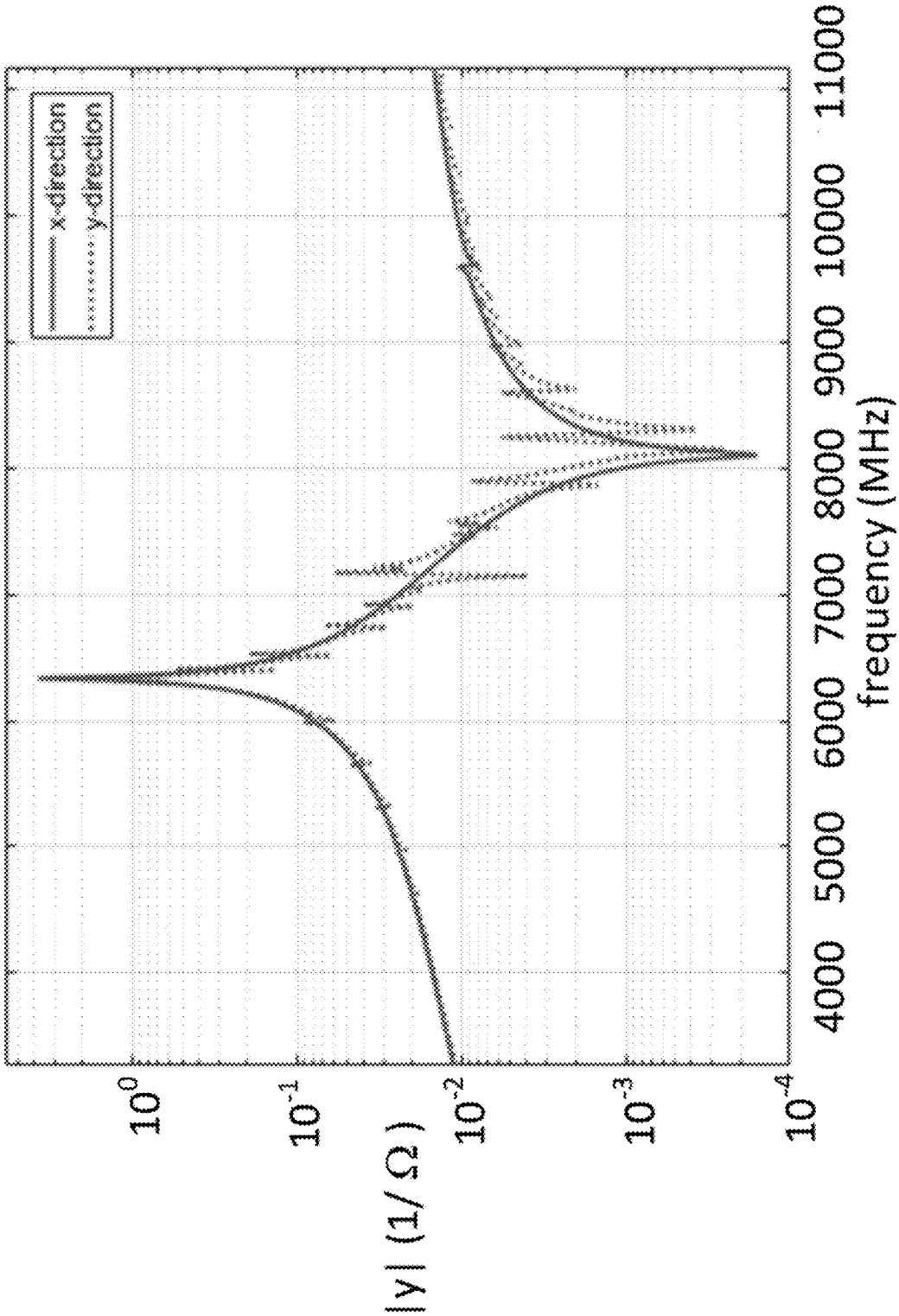
x-direction
y-direction
10^{0}
10^{-1}
10^{-2}
10^{-3}
10^{-4}
|y| (1/ Ω)
4000
5000
6000
7000
8000
9000
10000
11000
frequency (MHz)

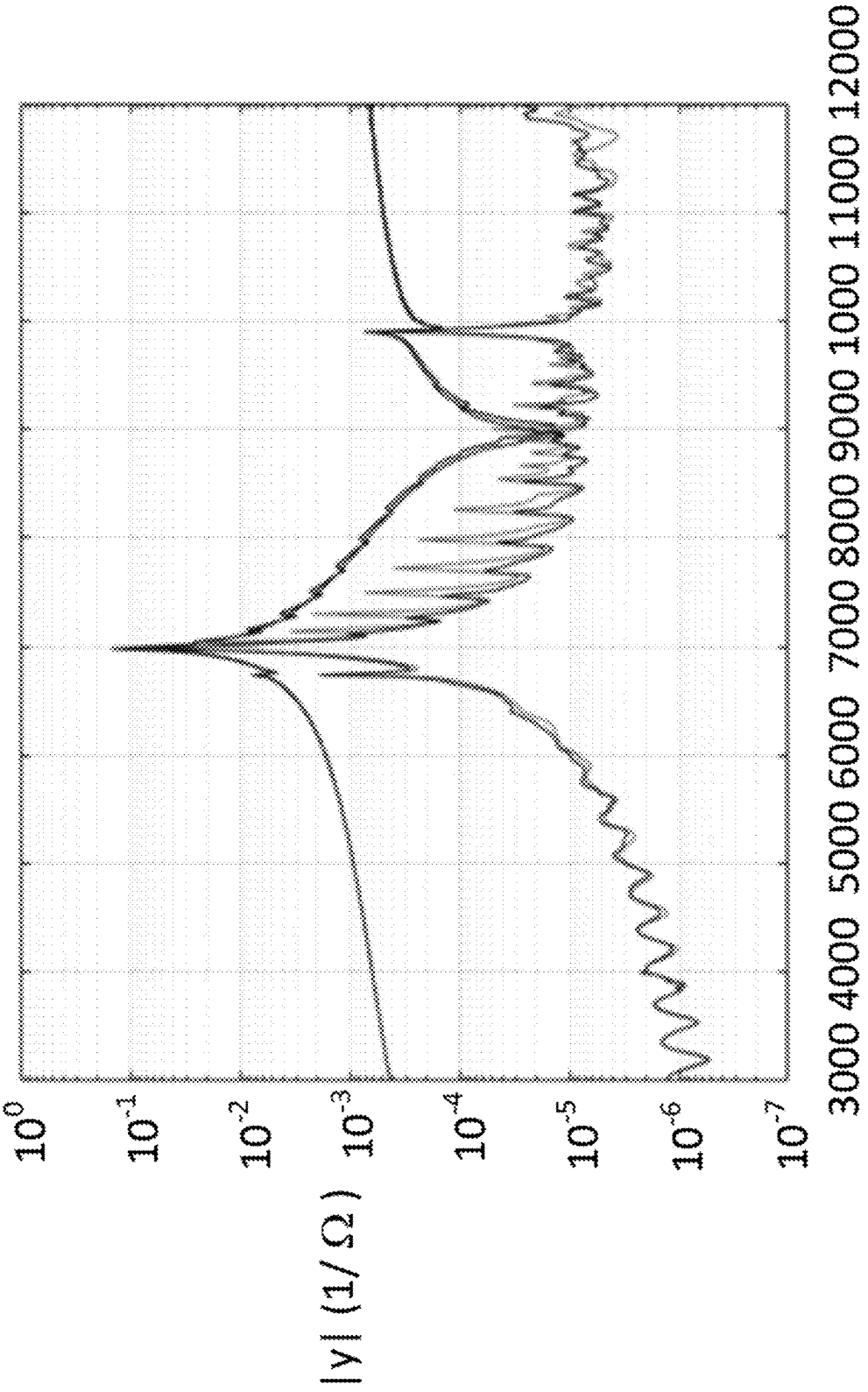
|y| (1/Ω)
10^0
10^-1
10^-2
10^-3
10^-4
10^-5
10^-6
10^-7
3000 4000 5000 6000 7000 8000 9000 1000 11000 12000
Frequency (MHz)

FIG. 9B

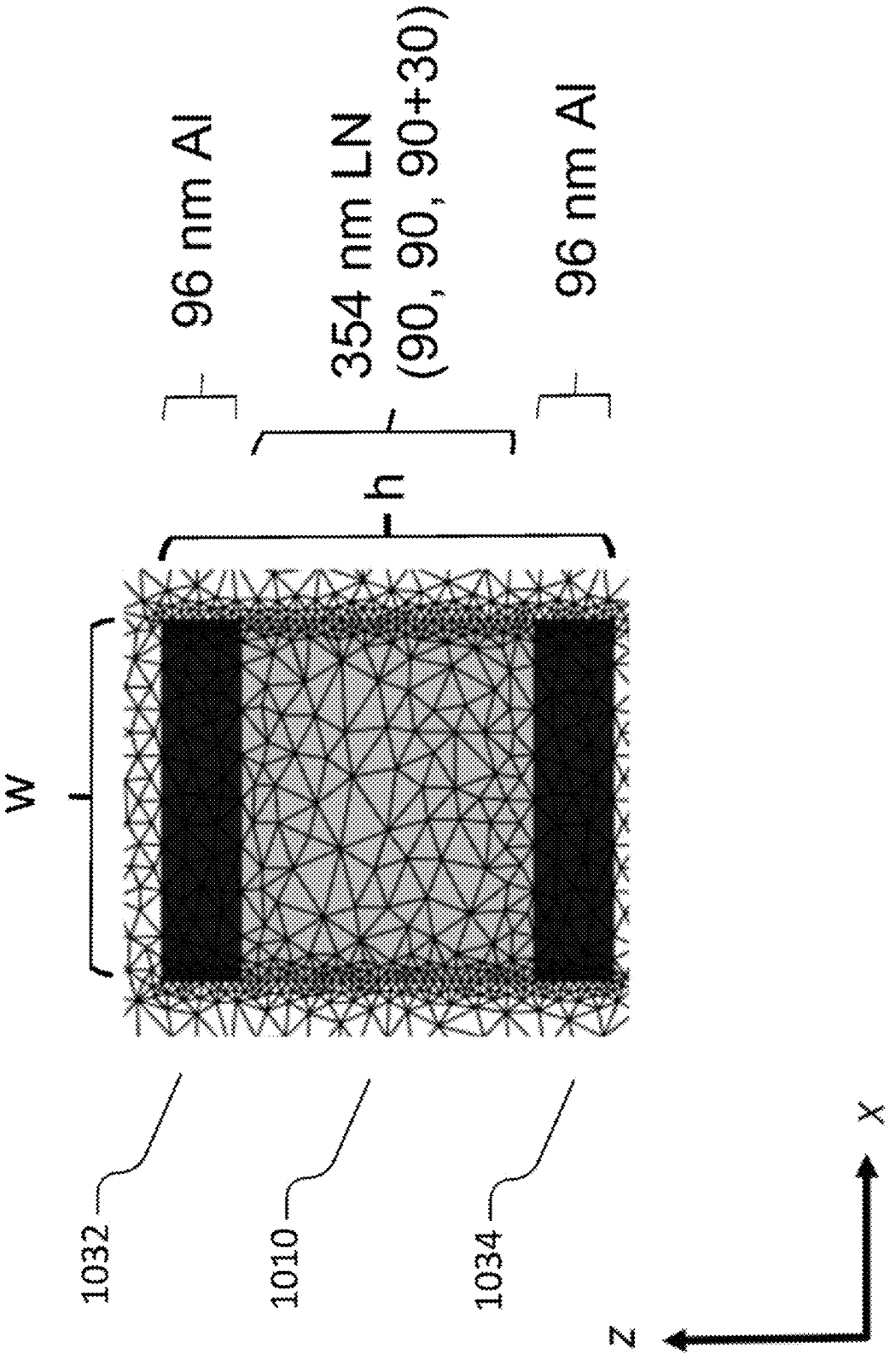

FIG. 10

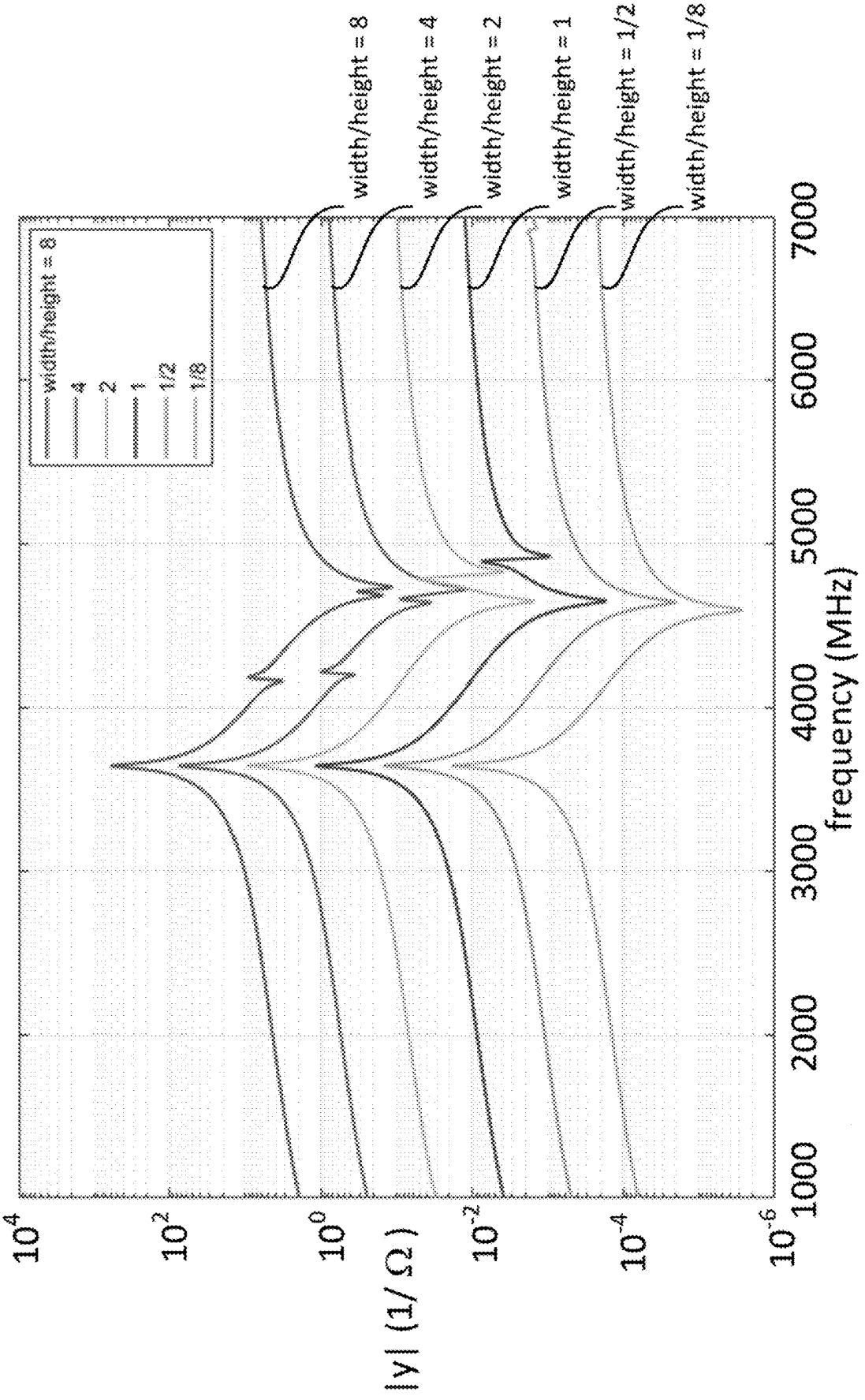
width/height = 8
4
2
1
1/2
1/8
width/height = 8
width/height = 4
width/height = 2
width/height = 1
width/height = 1/2
width/height = 1/8
10^4
10^2
10^0
10^{-2}
10^{-4}
10^{-6}
|y| (1/Ω)
1000
2000
3000
4000
5000
6000
7000
frequency (MHz)

FIG. 11A

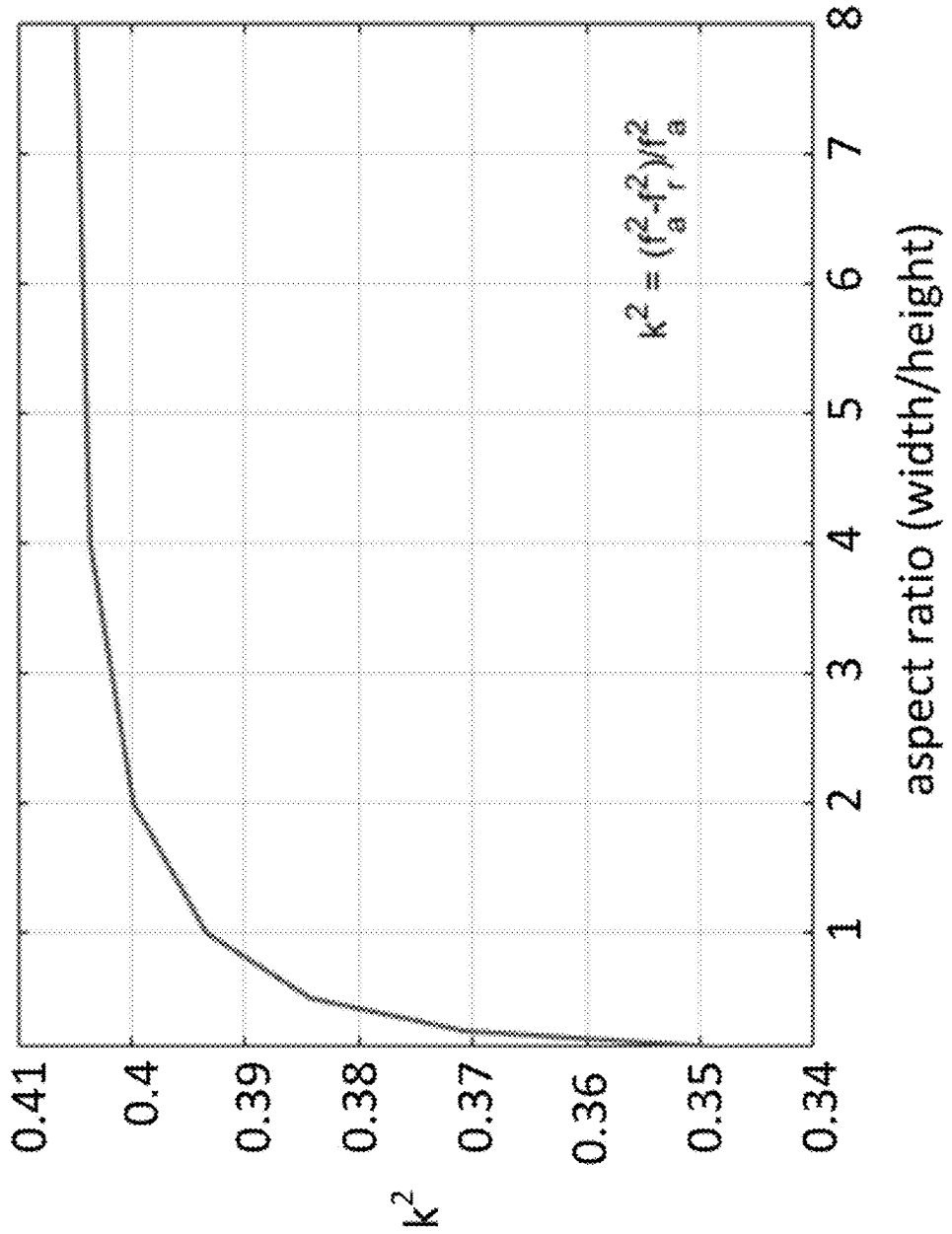
0.41
0.4
0.39
0.38
0.37
0.36
0.35
0.34
k²
1
2
3
4
5
6
7
8
aspect ratio (width/height)
k² = (r²a-r²r)/r²a

FIG. 11B

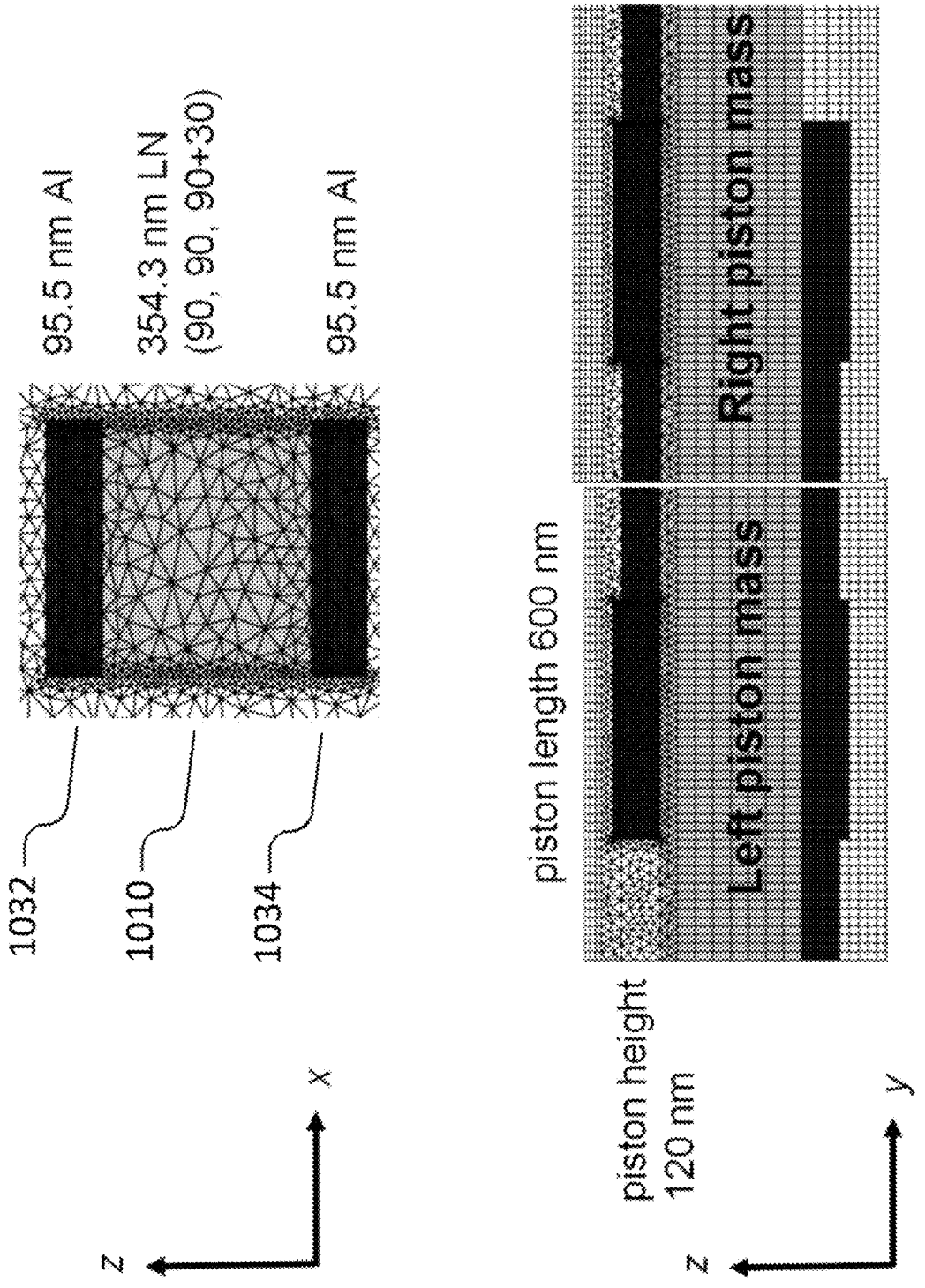
width 350 nm
95.5 nm Al
354.3 nm LN
(90, 90, 90+30)
95.5 nm Al
1032
1010
1034
z
x
piston length 600 nm
Right piston mass
Left piston mass
piston height
120 nm
z
y

FIG. 12A

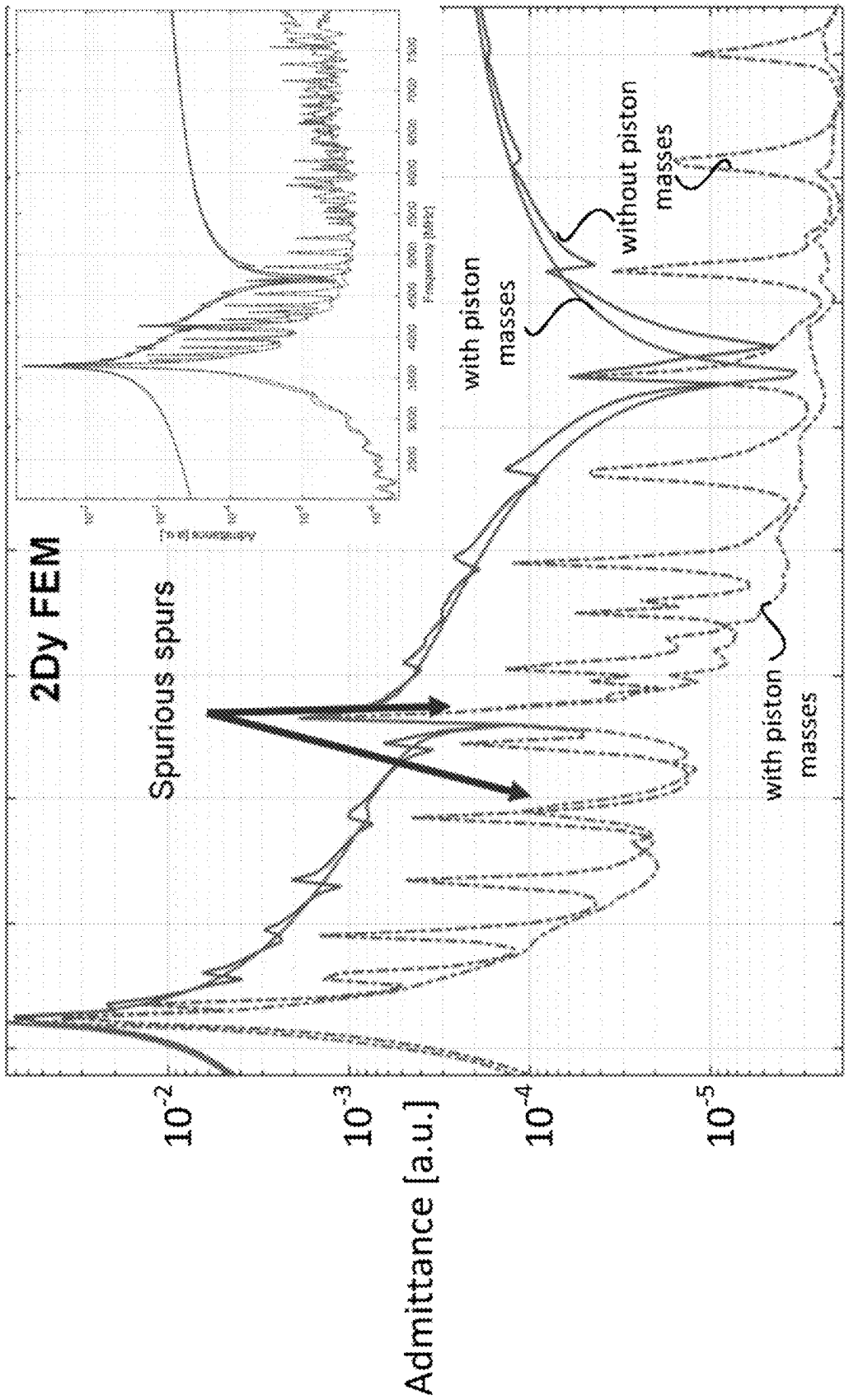
2Dy FEM
Spurious spurs
with piston masses
without piston masses
with piston masses
Admittance [a.u.]
Frequency (MHz)
3600
3800
4000
4200
4400
4600
4800
5000
5200

FIG. 12B

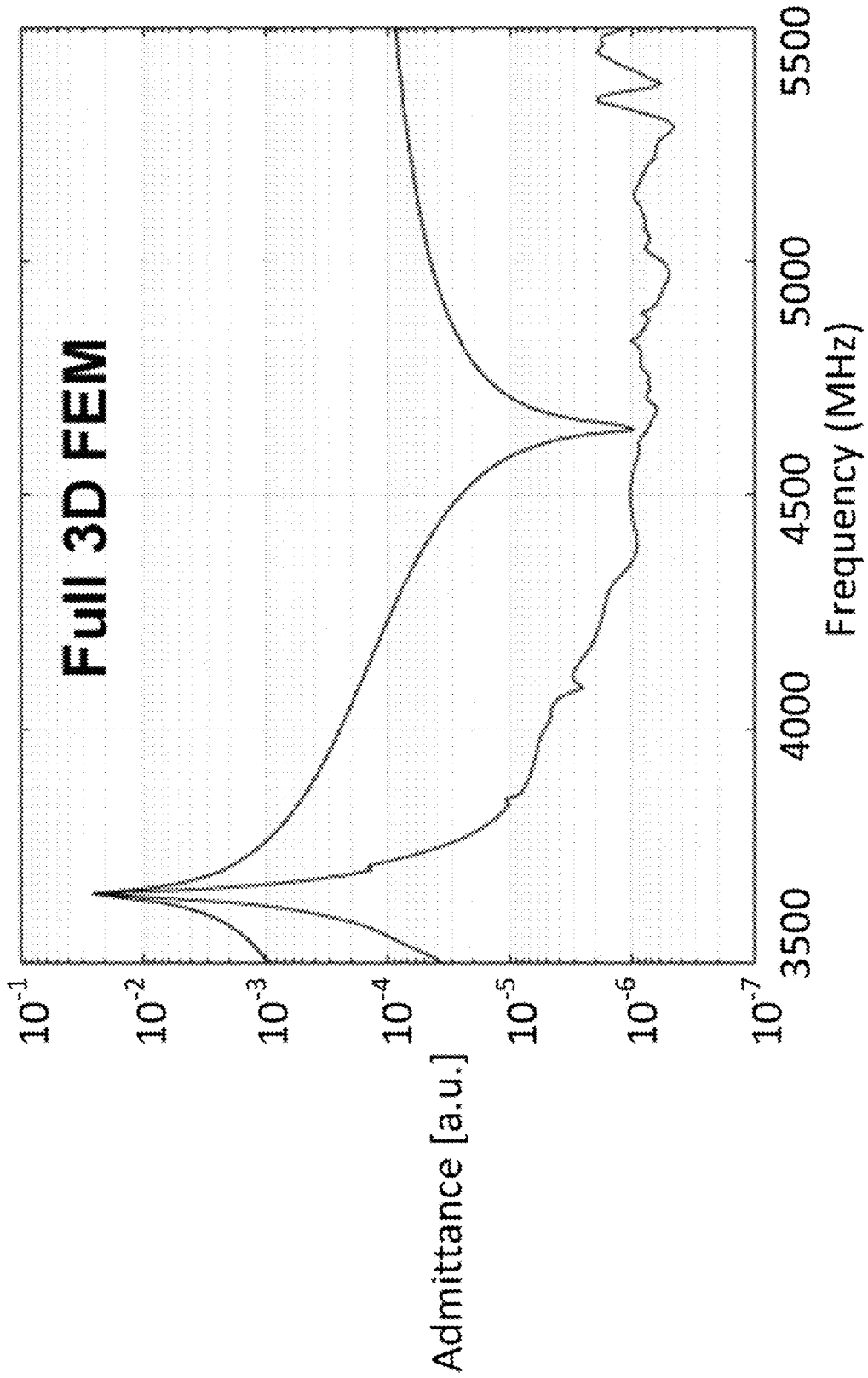
Full 3D FEM
Admittance [a.u.]
Frequency (MHz)
10^-1
10^-2
10^-3
10^-4
10^-5
10^-6
10^-7
3500
4000
4500
5000
5500

FIG. 12C

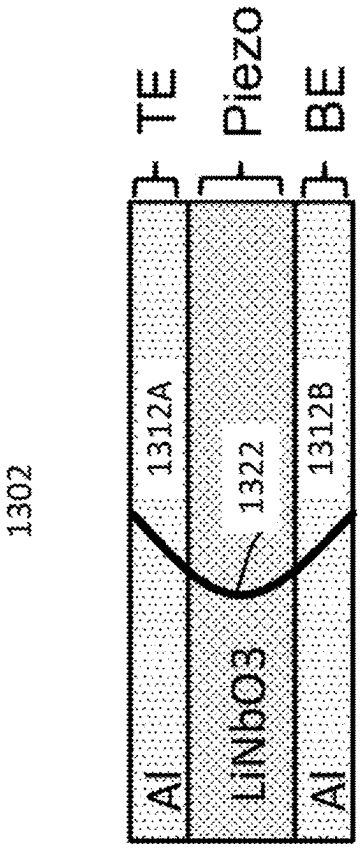

FIG. 13B

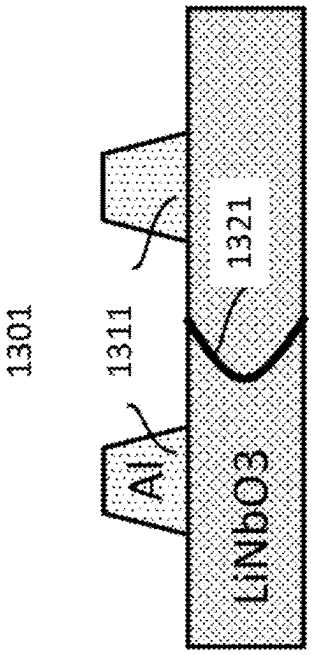

FIG. 13A

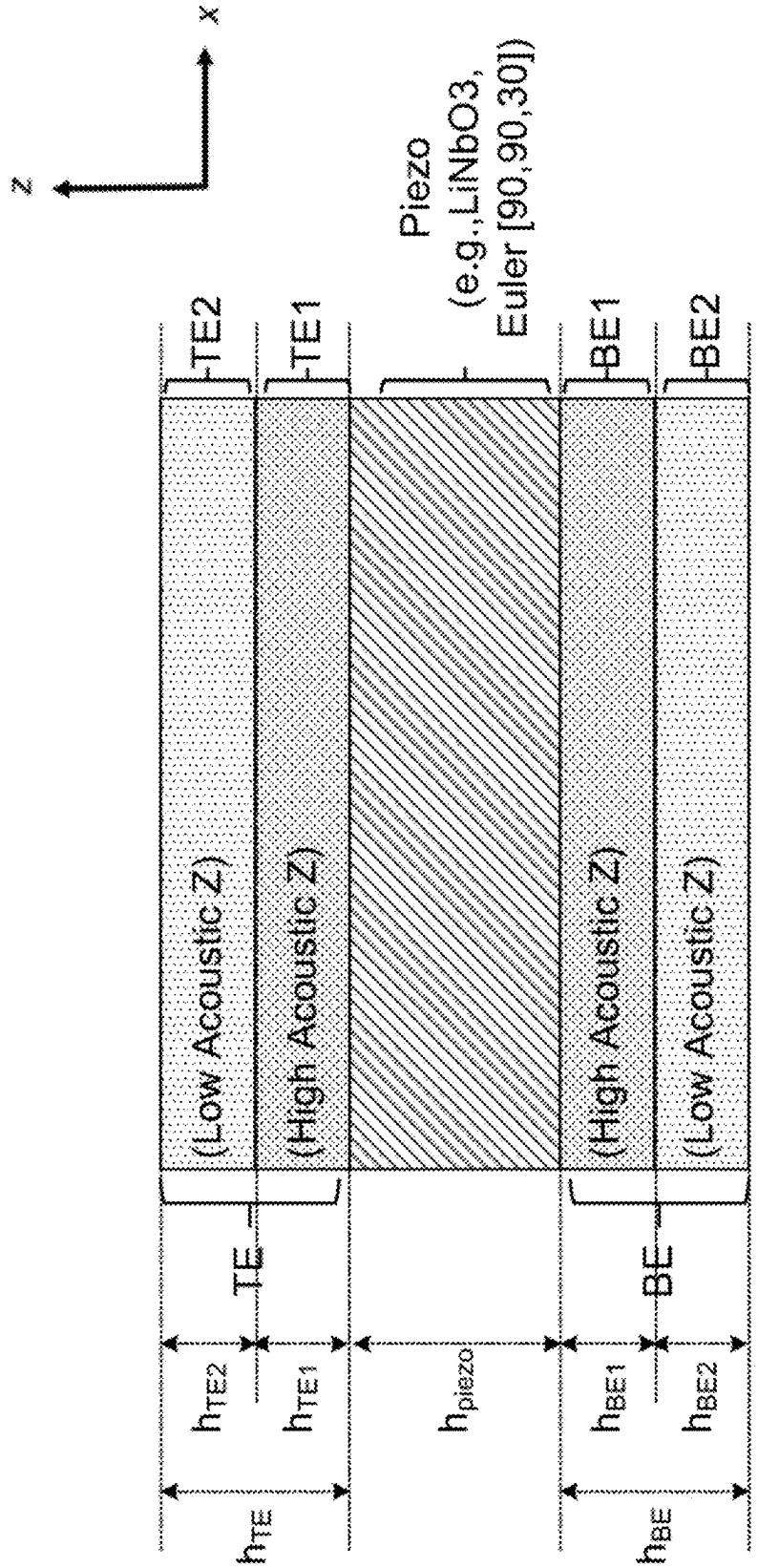
x
z
Piezo
(e.g.,LiNbO3,
Euler [90,90,30])
TE2
TE1
BE1
BE2
(Low Acoustic Z)
(High Acoustic Z)
(High Acoustic Z)
(Low Acoustic Z)
TE
BE
h_{TE2}
h_{TE1}
h_{piezo}
h_{BE1}
h_{BE2}
h_{TE}
h_{BE}

FIG. 14

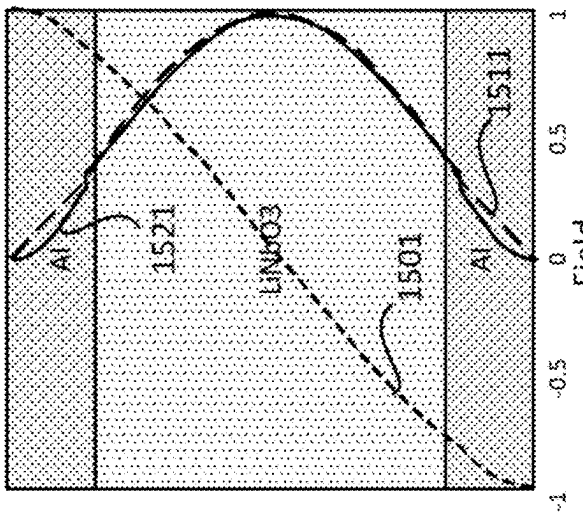

1-layer Electrode: Al

1531

FIG. 15A

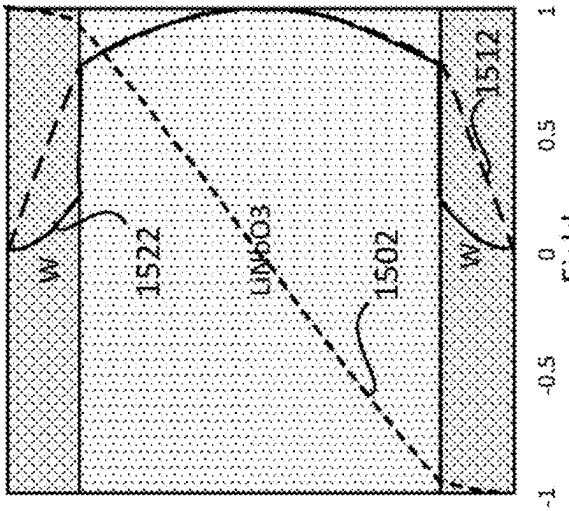

1-layer Electrode: W

1532

FIG. 15B

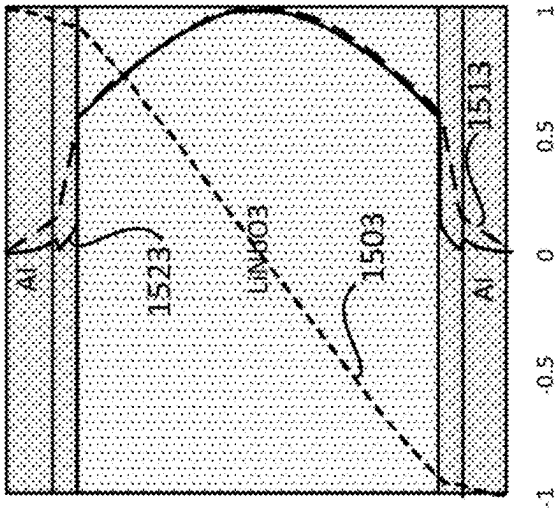

2-layer Electrode: W/Al

1533

FIG. 15C

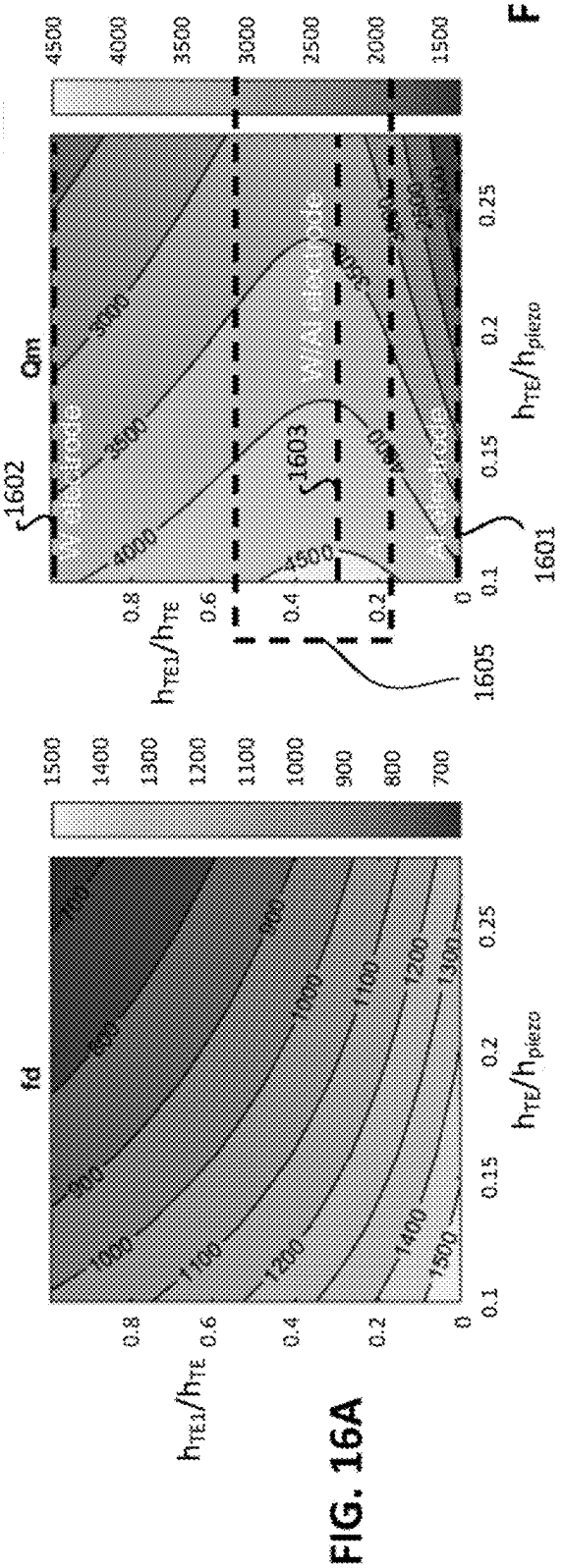

FIG. 16A

FIG. 16B

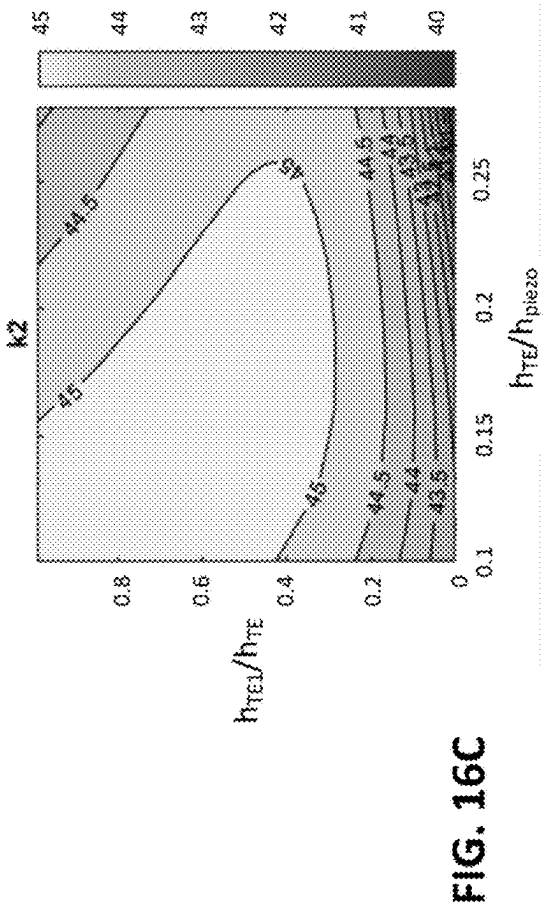

FIG. 16C

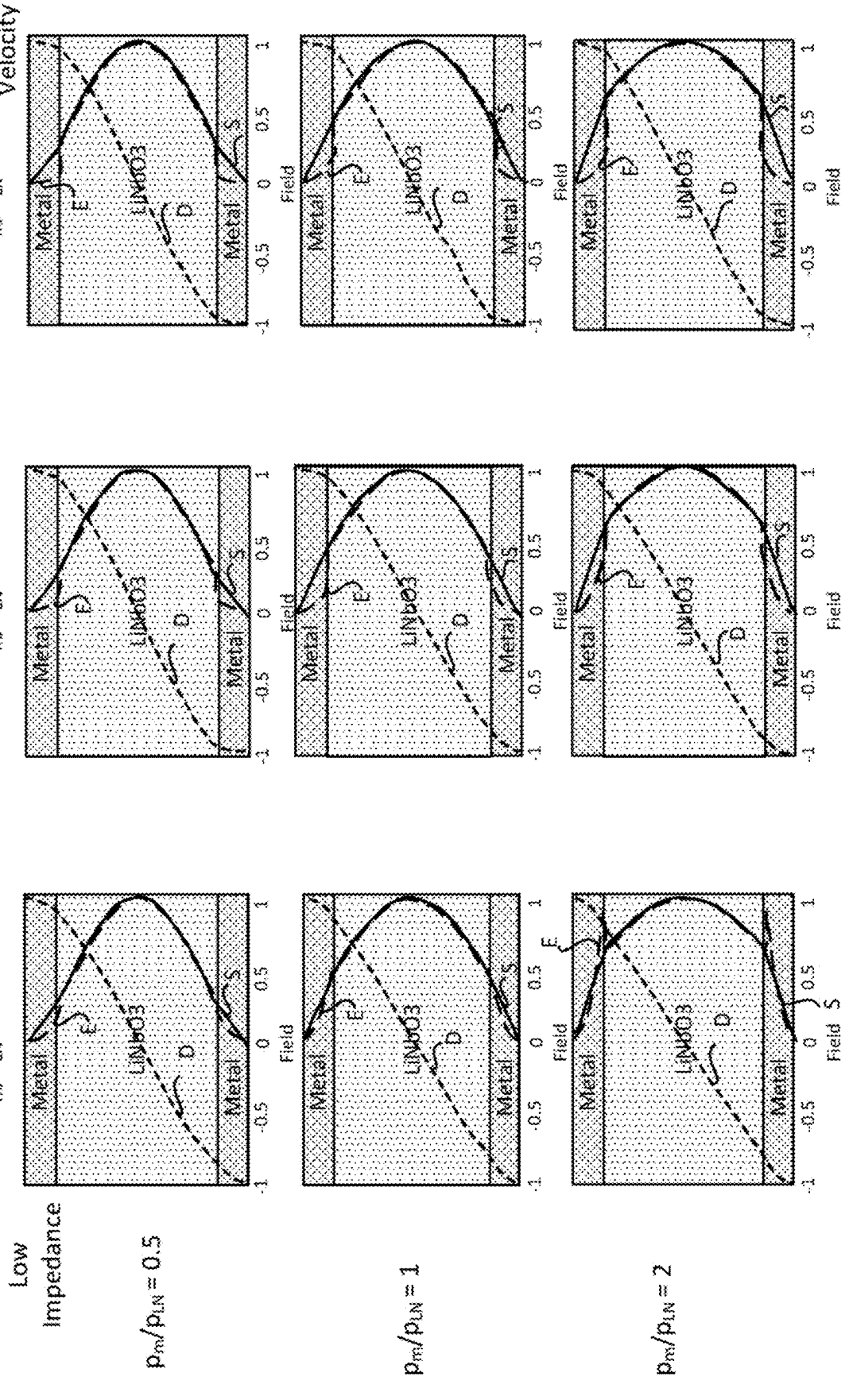
Low Impedance
High Velocity
$C_m/C_{LN} = 0.5$
$C_m/C_{LN} = 1$
$C_m/C_{LN} = 2$
$\rho_m/\rho_{LN} = 0.5$
$\rho_m/\rho_{LN} = 1$
$\rho_m/\rho_{LN} = 2$
Metal
LiNbO3
E
D
S
Field
-1
-0.5
0
0.5
1

FIG. 17

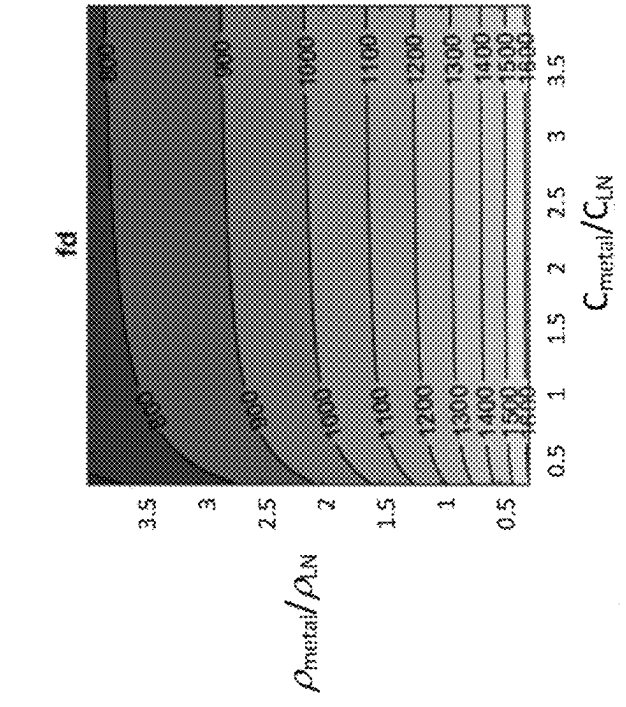

FIG. 18A

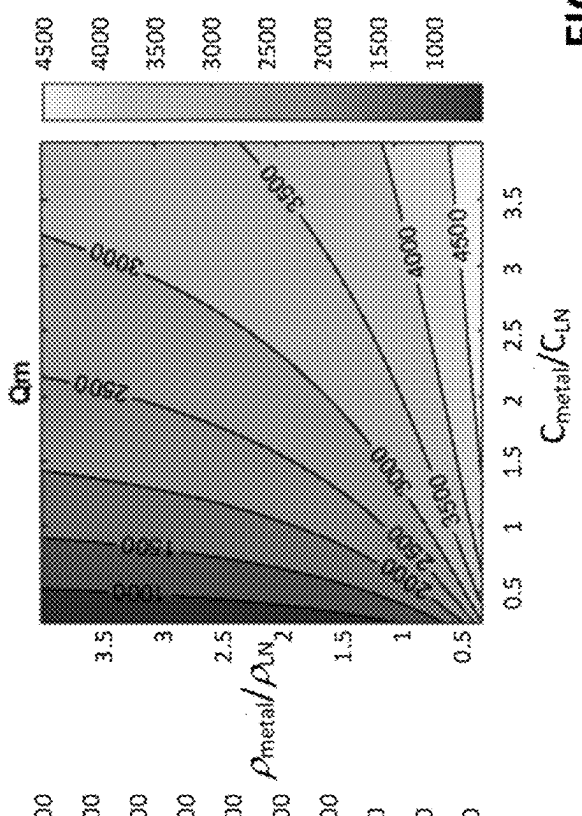

FIG. 18B

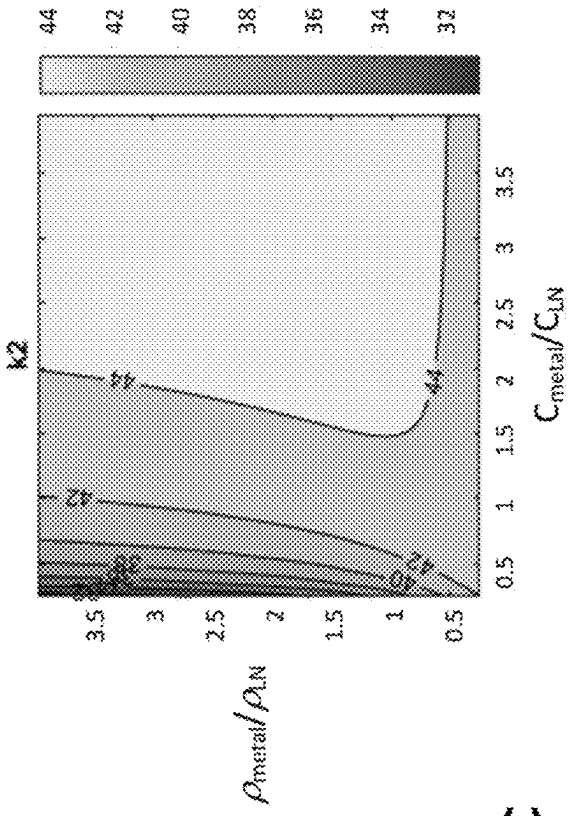

FIG. 18C

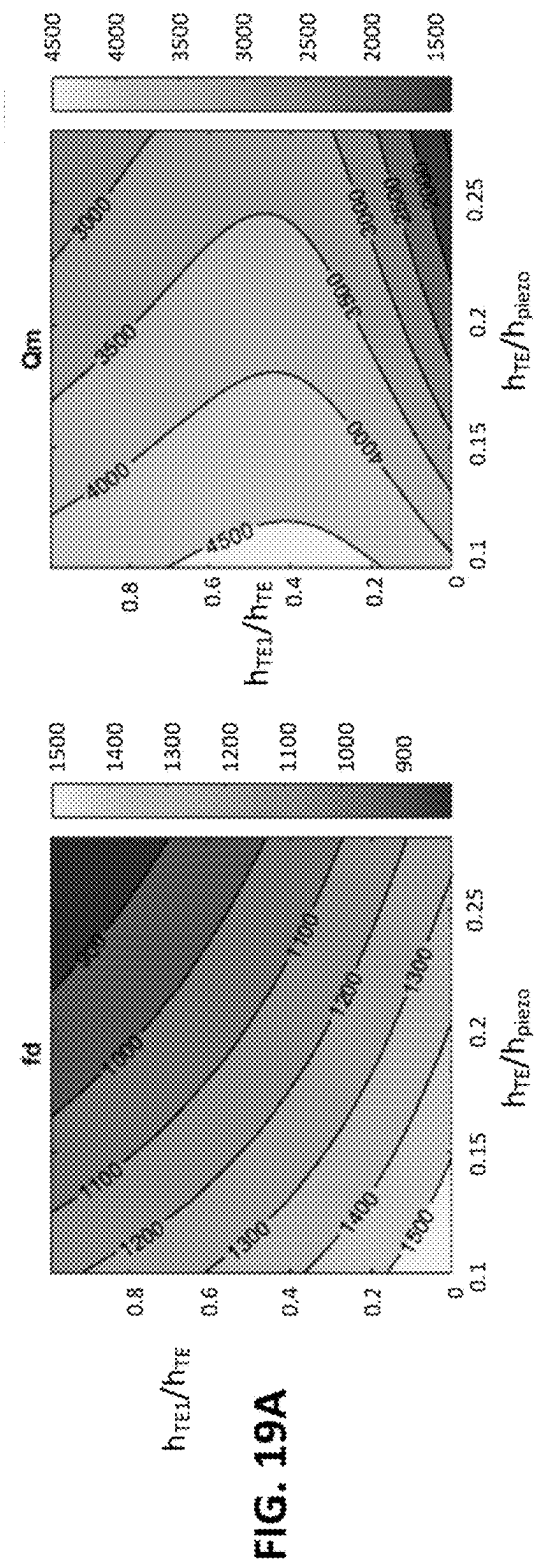

FIG. 19A

FIG. 19B

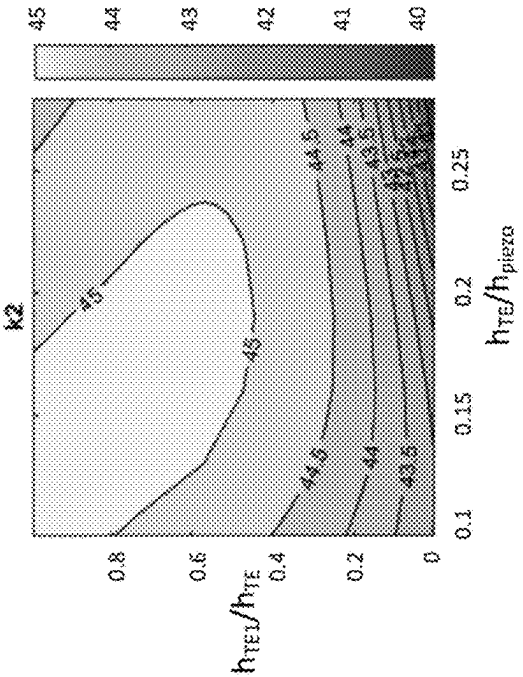

FIG. 19C

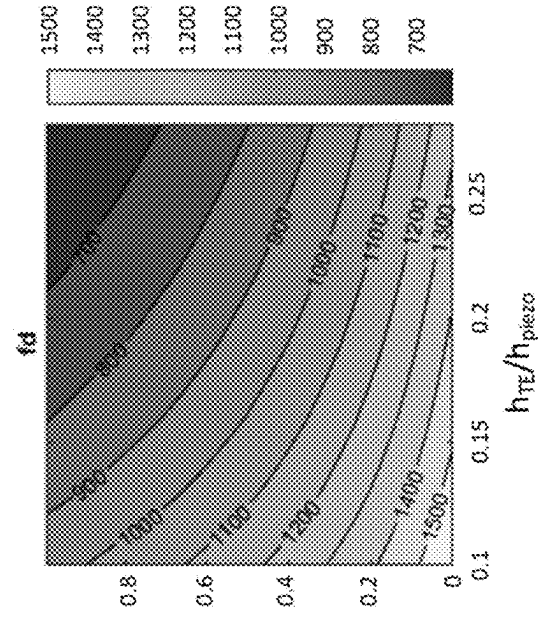

FIG. 20A

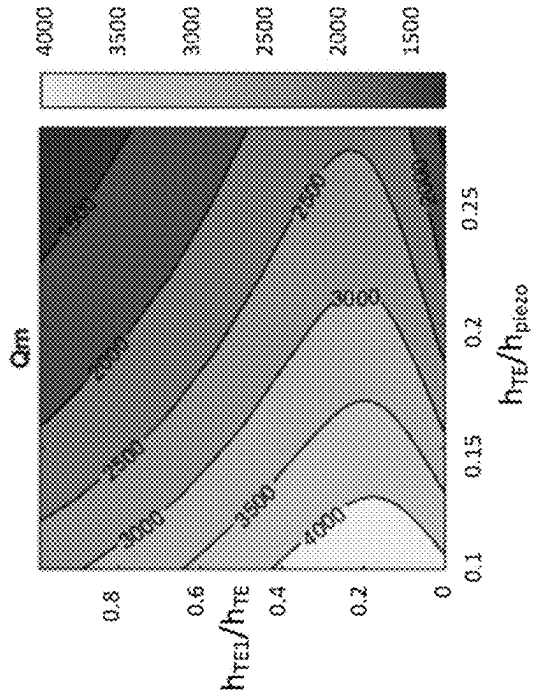

FIG. 20B

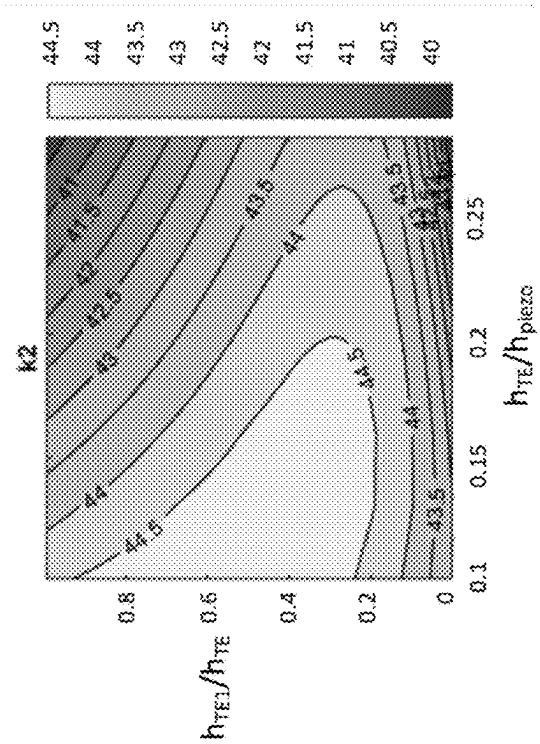

FIG. 20C

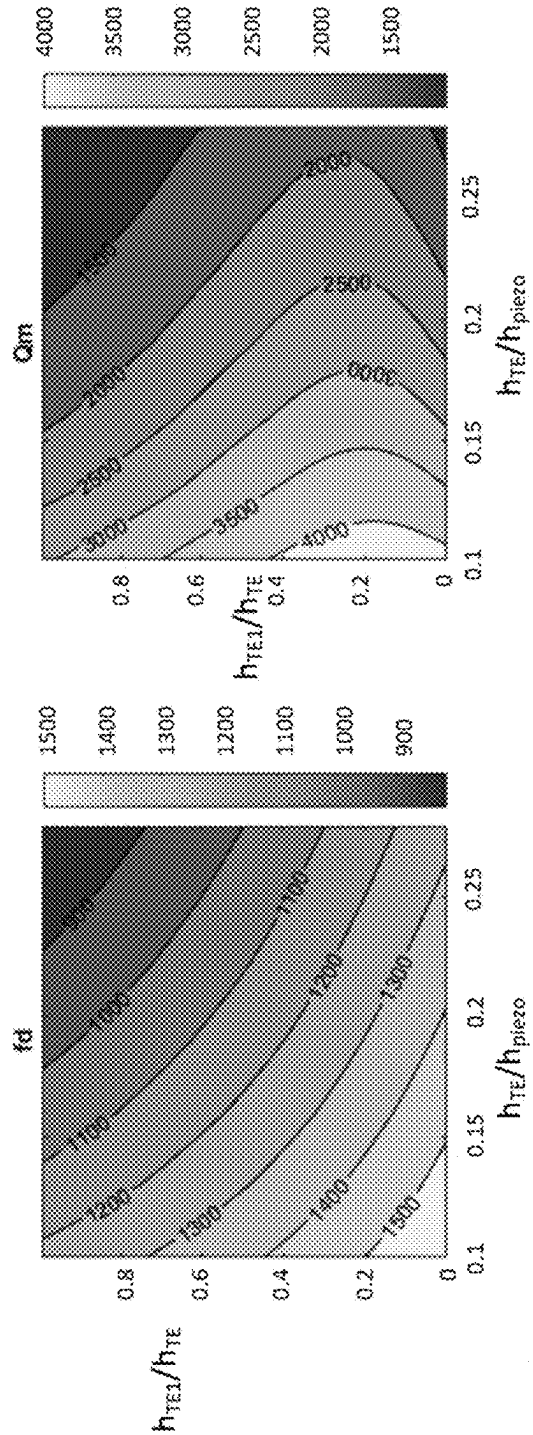

FIG. 21A

FIG. 21B

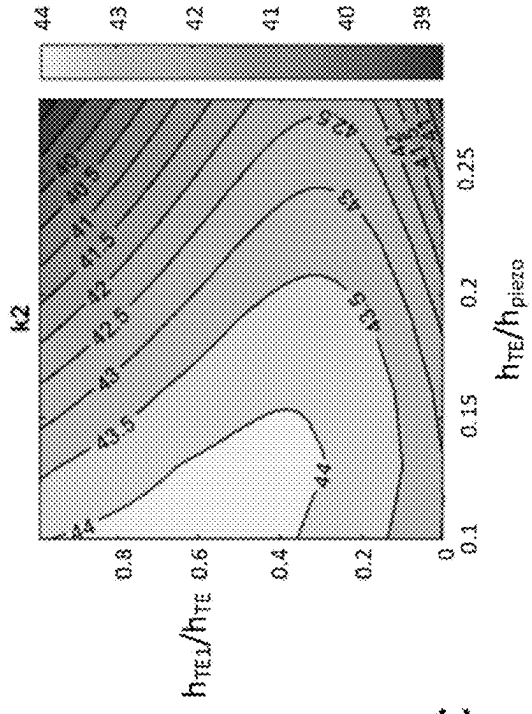

FIG. 21C

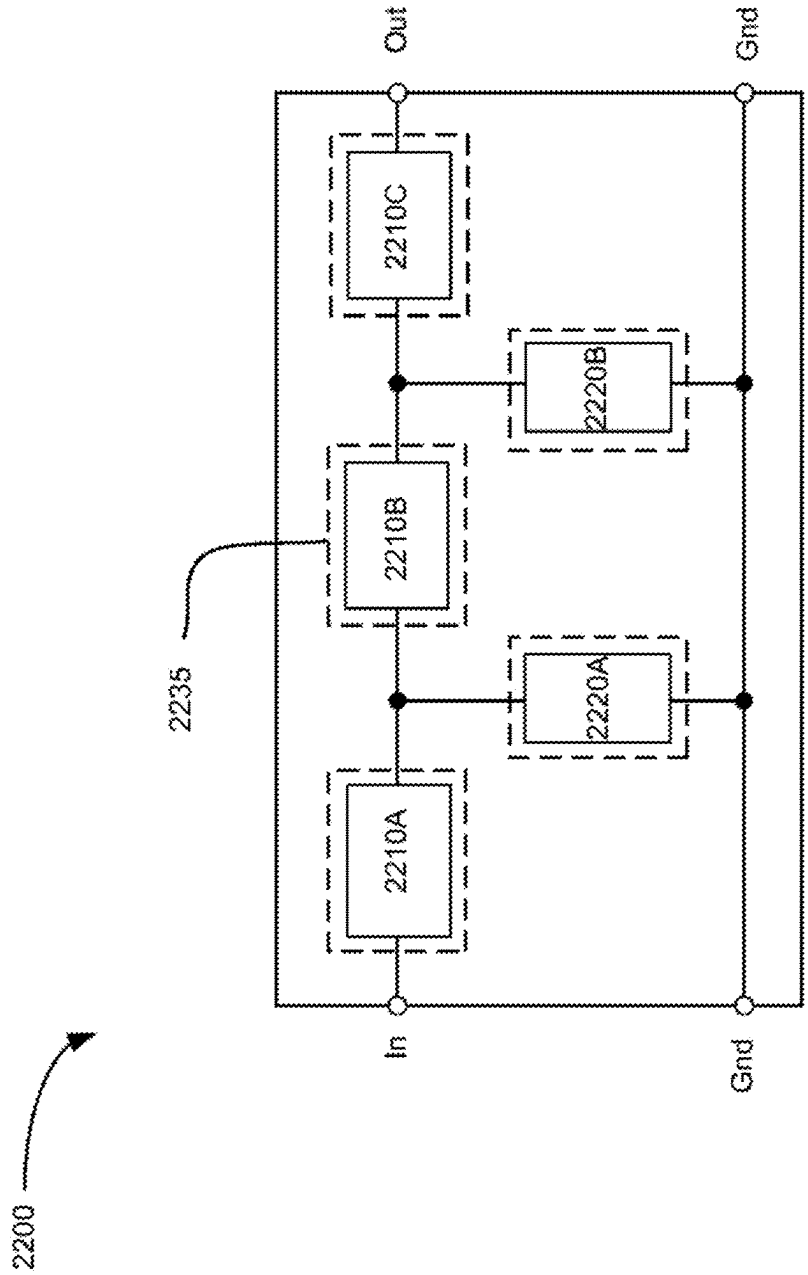

FIG. 22A

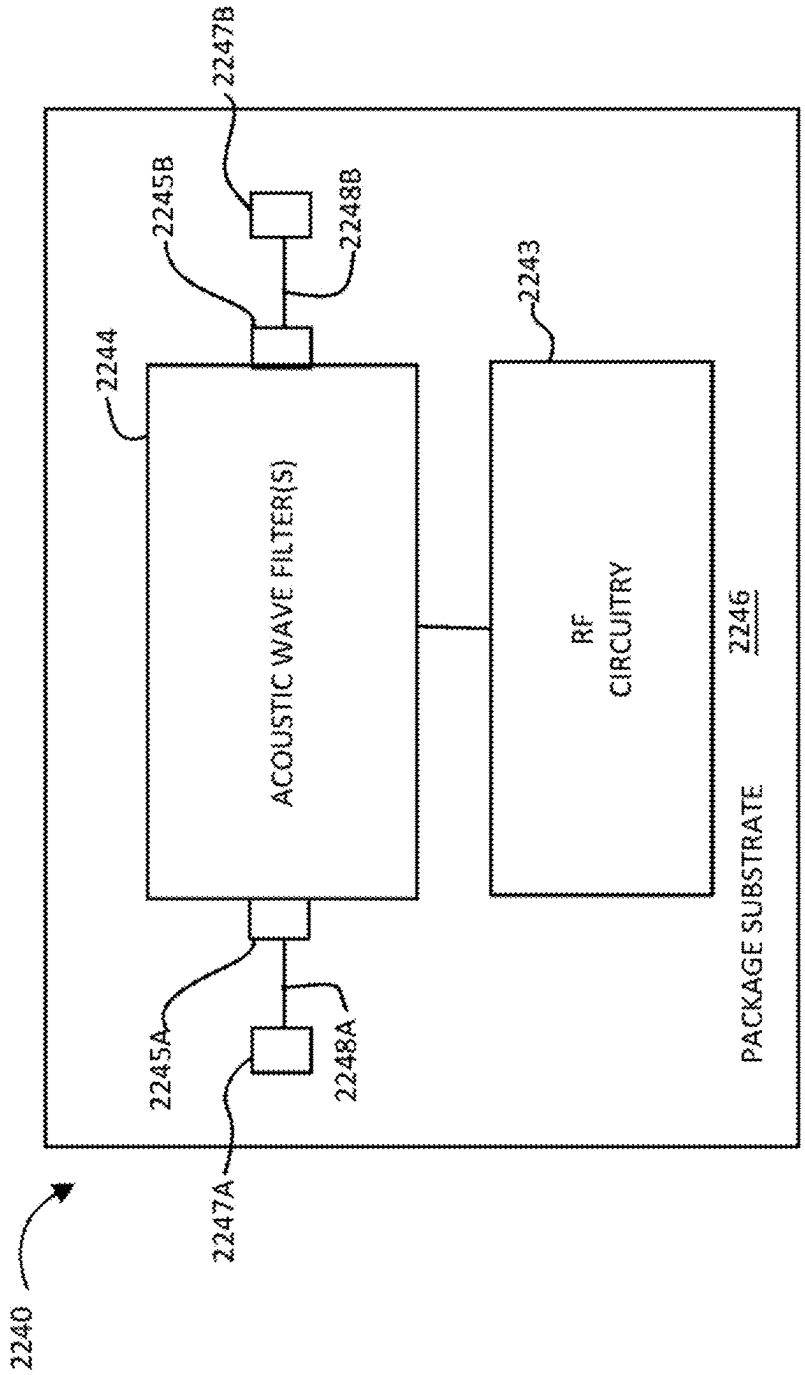
2240
MODULE
2247A
2245A
2248A
2244
ACOUSTIC WAVE FILTER(S)
2245B
2248B
2247B
2243
RF
CIRCUITRY
2246
PACKAGE SUBSTRATE

FIG. 22B

ACOUSTIC RESONATOR WITH ASPECT RATIO FOR SPUR REDUCTION

CROSS REFERENCE TO RELATED APPLICATIONS

[0001] The present application claims the benefit of priority to U.S. Provisional Patent Application No. 63/623,117 filed on Jan. 19, 2024, the entire contents of which are incorporated herein by reference.

TECHNICAL FIELD

[0002] This disclosure relates to film bulk acoustic resonators and also to filters including film bulk acoustic resonators for use in communications equipment.

BACKGROUND

[0003] A radio frequency (RF) filter is a two-port device configured to pass some frequencies and to stop other frequencies, where "pass" means transmit with relatively low signal loss and "stop" means block or substantially attenuate. The range of frequencies passed by a filter is referred to as the "passband" of the filter. The range of frequencies stopped by such a filter is referred to as the "stop-band" of the filter. A typical RF filter has at least one passband and at least one stop-band. Specific requirements on a passband or stop-band may depend on the specific application. For example, in some cases a "passband" may be defined as a frequency range where the insertion loss of a filter is better than a defined value such as 1 dB, 2 dB, or 3 dB, while a "stop-band" may be defined as a frequency range where the rejection of a filter is greater than a defined value such as 20 dB, 30 dB, 40 dB, or greater depending on application.

[0004] RF filters are used in communications systems where information is transmitted over wireless links. For example, RF filters may be found in the RF front ends of cellular base stations, mobile telephone and computing devices, satellite transceivers and ground stations, IoT (Internet of Things) devices, laptop computers and tablets, fixed point radio links, and other communications systems. RF filters are also used in radar and electronic and information warfare systems.

[0005] Performance enhancements to the RF filters in a wireless system can have a broad impact to system performance. Improvements in RF filters can be leveraged to provide system performance improvements, such as larger cell size, longer battery life, higher data rates, greater network capacity, lower cost, enhanced security, higher reliability, etc. These improvements can be realized at many levels of the wireless system both separately and in combination, for example, at the RF module, RF transceiver, mobile or fixed sub-system, or network levels. As the demand for RF filters operating at higher frequencies continues to increase, there is a need for improved filters that can operate at different frequency bands while also improving the manufacturing processes for making such filters.

SUMMARY

[0006] As noted above, resonator performance improvements, such as an improved Q factor, also have an improvement effect on the RF filters and network devices that include the improved resonator as described herein. Thus, according to an exemplary aspect, an acoustic resonator is provided to minimize spurs except at high frequencies by setting an aspect ratio of the electrode fingers of the acoustic resonator

[0007] Specifically, in an exemplary aspect, an acoustic resonator is provided that includes a plurality of nanowires that each include a piezoelectric layer having a first surface and a second surface; a first electrode on the first surface of the piezoelectric layer; and a second electrode on the second surface of the piezoelectric layer. In this aspect, the plurality of nanowires each extend from a first busbar predominantly in a first direction, such that a space is defined between a pair of nanowires of the plurality of nanowires in a second direction that is substantially perpendicular to the first direction, such that there is no piezoelectric material between the pair of nanowires in the second direction. Moreover, the plurality of nanowires each comprise a height in a thickness direction that is substantially orthogonal to the first and second directions, and the plurality of nanowires each comprises a ratio of a width in the second direction of at least one of the first electrode and the second electrode to the height of the nanowire that is less than 2.

[0008] In another exemplary aspect, the acoustic resonator includes a pair of busbars that includes the first busbar that is coupled to the first electrode of each of the plurality of nanowires and a second busbar that is coupled to the second electrode of each of the plurality of nanowires.

[0009] In another exemplary aspect of the acoustic resonator, the second electrode of each of the plurality of nanowires is a floating electrode.

[0010] In another exemplary aspect, the acoustic resonator includes a pair of piston masses disposed a top surface of the first electrode of each of the plurality of nanowires. In this aspect, the pair of piston masses can be disposed adjacent to a base and on a free end of each of the plurality of nanowires.

[0011] In another exemplary aspect of the acoustic resonator, the first electrode of each of the plurality of nanowires comprises multiple layers of electrodes in the thickness direction, and the multiple layers of electrodes of the first electrode include a first electrode layer having a first acoustic impedance and a second electrode layer having a second acoustic impedance that is lower than the first acoustic impedance. Moreover, the second electrode of each of the plurality of nanowires comprises multiple layers of electrodes in the thickness direction, and the multiple layers of electrodes of the second electrode include a first electrode layer having a first acoustic impedance and a second electrode layer having a second acoustic impedance that is lower than the first acoustic impedance of the first electrode layer of the second electrode.

[0012] In another exemplary aspect of the acoustic resonator, a number of the multiple layers of electrodes of the first electrode is 2, and a number of the multiple layers of electrodes of the second electrode is 2.

[0013] In another exemplary aspect of the acoustic resonator, the first electrode layer of the first electrode is disposed between the second electrode layer of the first electrode and the piezoelectric layer, and the first electrode layer of the second electrode is disposed between the second electrode layer of the second electrode and the piezoelectric layer.

[0014] In another exemplary aspect of the acoustic resonator, a ratio of a thickness of the first electrode layer of the first electrode to a thickness of the multiple layers of electrodes of the first electrode is between 0.1 to 0.6.

Moreover, a ratio of a thickness of the first electrode layer of the second electrode to a thickness of the multiple layers of electrodes of the second electrode is between 0.1 to 0.6.

[0015] In another exemplary aspect of the acoustic resonator, a ratio of a thickness of the multiple layers of electrodes of the first electrode to a thickness of the piezoelectric layer is between 0.1 to 0.5. Moreover, a ratio of a thickness of the multiple layers of electrodes of the second electrode to a thickness of the piezoelectric layer is between 0.1 to 0.5.

[0016] In another exemplary aspect, an acoustic resonator is provided that includes a plurality of electrode fingers that each include a piezoelectric layer having a first surface and a second surface; a top electrode on the first surface of the piezoelectric layer; and a bottom electrode on the second surface of the piezoelectric layer. In this aspect, the top electrode of the plurality of electrode fingers each extend from a first busbar predominantly in a first direction, wherein a space is defined between a pair of electrode fingers in a second direction that is substantially perpendicular to the first direction such that there is no piezoelectric material between the pair of nanowires in the second direction. Moreover, the plurality of electrode fingers each comprise a width in the second direction and a total height in a thickness direction that is substantially orthogonal to the first and second directions, and at least one finger of the plurality of electrode fingers comprises a ratio of the to the total height that is less than 2.

[0017] In another exemplary aspect, a bandpass filter is provided that includes a plurality of acoustic resonators comprising one or more series resonators and one or more shunt resonators, at least one acoustic resonator of the plurality of acoustic resonators including a plurality of nanowires that each include a piezoelectric layer having a first surface and a second surface; a first electrode on the first surface of the piezoelectric layer; and a second electrode on the second surface of the piezoelectric layer. In this aspect, the plurality of nanowires each extend from a first busbar predominantly in a first direction, such that a space is defined between a pair of nanowires of the plurality of nanowires in a second direction that is substantially perpendicular to the first direction, such that there is no piezoelectric material between the pair of nanowires in the second direction, the nanowires each comprise a height in a thickness direction that is substantially orthogonal to the first and second directions, and the plurality of nanowires each comprises a ratio of a width in the second direction of at least one of the first electrode and the second electrode to the height of the nanowire that is less than 2.

BRIEF DESCRIPTION OF THE DRAWINGS

[0018] The accompanying drawings, which are incorporated into and form a part of this specification, illustrate one or more example aspects of the present disclosure and, together with the detailed description, serve to explain their principles and implementations.

[0019] FIG. **1** illustrates a schematic plan view and schematic cross-sectional views of a Y-cut film bulk acoustic resonator (YBAR) according to an exemplary aspect.

[0020] FIG. **2**A illustrates a schematic plan view and schematic cross-sectional views of a YBAR according to another exemplary aspect.

[0021] FIG. **2**B illustrates a schematic plan view and schematic cross-sectional views of a variation of the YBAR shown in FIG. **2**A according to another exemplary aspect.

[0022] FIG. **3**A is a schematic cross-sectional view of a YBAR according to an exemplary aspect.

[0023] FIG. **3**B is an alternative schematic cross-sectional view of a YBAR according to an exemplary aspect.

[0024] FIG. **4**A illustrates a schematic plan view and a perspective view of an acoustic resonator structure that is a refinement of the exemplary aspect of the YBAR shown in FIG. **2**A. FIG. **4**B illustrates a cross-section view of the IDT configuration in FIG. **4**A.

[0025] FIG. **5** illustrates a schematic plan view and a perspective view of an IDT configuration of another refinement of the exemplary aspect of the YBAR shown in FIG. **2**A.

[0026] FIG. **6** illustrates a top view of the IDT configuration in FIGS. **4**A and **4**B according to an exemplary aspect.

[0027] FIGS. **7**A and **7**B illustrate graphs of an admittance [y] as a function of frequency of a the acoustic resonator according to an exemplary aspect.

[0028] FIG. **8** illustrates a top view of another IDT configuration of the acoustic resonators shown FIGS. **4**A and **4**B according to an exemplary aspect.

[0029] FIGS. **9**A and **9**B illustrate graphs of an admittance [y] as a function of frequency of an acoustic resonator as shown in FIG. **8** according to an exemplary aspect.

[0030] FIG. **10** illustrates a cross-sectional view of an IDT finger of an acoustic resonator configuration as shown in either FIG. **4**A and/or FIG. **5** according to exemplary aspects.

[0031] FIG. **11**A illustrates a graph of an admittance [y] as a function of frequency of an acoustic resonators according to an exemplary aspect.

[0032] FIG. **11**B illustrates a graph of the coupling coefficient as a function of an aspect ratio of an acoustic resonators according to an exemplary aspect.

[0033] FIG. **12**A illustrates a cross-sectional view of an IDT finger of an acoustic resonator configuration as shown in FIG. **8** according to an exemplary aspect.

[0034] FIGS. **12**B and **12**C illustrate graphs of an admittance [y] as a function of frequency of an acoustic resonator according to an exemplary aspect.

[0035] FIGS. **13**A-**13**B compare energy/acoustic damping in metal layers according to an aspect of the disclosure.

[0036] FIG. **14** shows an example of a multi-layer metal structure for a first conductor pattern disposed on a first surface of a piezoelectric layer and for a second conductor pattern disposed on a second surface of the piezoelectric layer of an acoustic resonator structure according to an aspect of the disclosure.

[0037] FIGS. **15**A-**15**C show displacements, stresses, and energies of three electrode structures, respectively according to an aspect of the disclosure.

[0038] FIGS. **16**A-**16**C show an fd plot, a Qm plot, and a k2 plot, respectively, for an acoustic resonator ARN that has a 2-layer electrode structure shown in FIG. **14** according to an aspect of the disclosure.

[0039] FIG. **17** shows simulated results of displacements ("D"), stresses ("S"), and energies ("E") of nine electrode structures, respectively according to an aspect of the disclosure.

[0040] FIG. **18**A shows an fd plot indicating how the parameter fd varies with C_m/C_{LN} and ρ_m/ρ_{LN} according to an aspect of the disclosure.

[0041] FIG. **18**B shows a Qm plot indicating how the parameter Qm varies with C_m/C_{LN} and ρ_m/ρ_{LN} according to an aspect of the disclosure.

[0042] FIG. **18**C shows a k2 plot indicating how the parameter k2 varies with C_m/C_{LN} and ρ_m/ρ_{LN} according to an aspect of the disclosure.

[0043] FIGS. **19**A-**19**C, **20**A-**20**C, and **21**A-**21**C show the effect of different metal materials as TE1 and BE1 according to an aspect of the disclosure.

[0044] FIG. **22**A is a schematic block diagram of a filter using acoustic resonators according to an exemplary aspect.

[0045] FIG. **22**B is a schematic diagram of a radio frequency module that includes an acoustic wave filter of FIG. **22**A according to an exemplary aspect.

[0046] Throughout this description, elements appearing in figures are assigned three-digit or four-digit reference designators, where the two least significant digits are specific to the element and the one or two most significant digit is the figure number where the element is first introduced. An element that is not described in conjunction with a figure may be presumed to have the same characteristics and function as a previously-described element having the same reference designator.

DETAILED DESCRIPTION

[0047] Various aspects of the disclosed film bulk acoustic resonator, filter device and method of manufacturing the same are now described with reference to the drawings, wherein like reference numerals are used to refer to like elements throughout. In the following description, for purposes of explanation, numerous specific details are set forth in order to promote a thorough understanding of one or more aspects of the disclosure. It may be evident in some or all instances, however, that any aspects described below can be practiced without adopting the specific design details described below. In other instances, well-known structures and devices are shown in block diagram form in order to facilitate description of one or more aspects. The following presents a simplified summary of one or more aspects of the invention in order to provide a basic understanding thereof.

[0048] FIG. **1** shows a simplified top view and a cross-sectional view of a Y-cut film bulk acoustic resonator (YBAR) **100** according to an exemplary aspect. According to this aspect, the YBAR **100** includes a piezoelectric layer **110** (piezoelectric plate or piezoelectric layer may be used interchangeably) having essentially parallel front and back surfaces **112**, **114**, respectively. In this context, "essentially parallel" means "as close to parallel as possible" or "parallel within reasonable manufacturing tolerances." Thus, it should be appreciated that the term "parallel" generally refers to the front side **112** and back side **114** opposing each other and that the surfaces may not be strictly planar and parallel to each other in an exemplary aspect. For example, due to the manufacturing variances resulting from the deposition process, the front side **112** and back side **114** may have undulations of the surface as would be appreciated to one skilled in the art. In addition, the piezoelectric layer **110** can be a thin single-crystal layer of a piezoelectric material. The term "single-crystal" does not necessarily mean entirely of a uniform crystalline structure and may include impurities due to manufacturing variances as long as the crystal structure is within acceptable tolerances.

[0049] According to the exemplary aspect, the piezoelectric layer **110** is preferably lithium niobate (LN), but may be lithium tantalate (LT), lanthanum gallium silicate, gallium nitride, or some other material. The piezoelectric layer **110** is cut such that the orientation of the X, Y, and Z crystalline axes with respect to the front and back surfaces is known and consistent.

[0050] In an exemplary aspect, the thickness ts of the piezoelectric layer **110** may be determined from:

$$ts \approx n * V_{SH}/2F_R,$$

where F_R is a desired operation frequency, VSH is the shear wave velocity of the piezoelectric layer, and n=1, 3, 5, . . . is the desired mode (overtone) number. In this regard, n=1 is usually referred to as "fundamental mode" and n>1 are referred to as "overtones".

[0051] The back side **114** of the piezoelectric layer **110** is attached to a substrate **120** that provides mechanical support to the piezoelectric layer **110**. The substrate **120** may be, for example, silicon, sapphire, quartz, or some other material. The piezoelectric layer **110** may be bonded to the substrate **120** using a wafer bonding process, or grown on the substrate **120**, or attached to the substrate in some other manner. The piezoelectric layer **110** may be attached directly to the substrate or may be attached to the substrate via one or more intermediate material layers as discussed below with respect to FIGS. **3**A and **3**B. In other words, the back side **114** of the piezoelectric layer **110** can be coupled or connected either directly or indirectly, via one or more intermediate layers (e.g., a dielectric layer), to a surface of the substrate **120**. Moreover, the phrase "supported by" or "attached" may, as used herein interchangeably, means attached directly, attached indirectly, mechanically supported, structurally supported, or any combination thereof.

[0052] A cavity **125** is formed in the substrate **120** such that the portion of the piezoelectric layer **110** containing the front-side and back-side conductor patterns **130**, **132**, **134** is suspended over the cavity **125**. The portion of the piezoelectric layer **110** that is over (e.g., spanning or extending over) the cavity can be referred to herein as a "diaphragm" due to its physical resemblance to the diaphragm of a microphone. The diaphragm can be contiguous with the rest of the piezoelectric layer **110** around all of a perimeter of the cavity **125**. In this context, "contiguous" means "continuously connected without any intervening item". However, the diaphragm can be configured with at least 50% of the edge surface of the diaphragm coupled to the edge of the piezoelectric layer **110** in an exemplary aspect.

[0053] According to an exemplary aspect, "cavity" has its conventional meaning of "an empty space within a solid body." The cavity **125** may be a hole completely through the substrate **120** (as shown in Section A-A) or a recess in the substrate **120** that does not extend through the substrate **120**. The cavity **125** may be formed, for example, by selective etching of the substrate **120** before or after the piezoelectric layer **110** and the substrate **120** are attached. In some cases, the cavity **125** is not formed in the substrate **120**, but instead the cavity is formed in one or more intermediate layers between the piezoelectric layer **110** and the substrate **120**. In

some cases, the cavity **120** is only partially formed in the substrate **120** and may also partially formed in one or more intermediate layers between the piezoelectric layer **110** and the substrate **120**. Moreover, as shown in FIG. **1**, the cavity **125** has a rectangular shape. However, the cavity of YBAR **100** may have a different shape, such as a regular or irregular polygon. The cavity of YBAR **100** may more or fewer than four sides, which may be straight or curved.

[0054] A first front-side conductor pattern **130** (e.g., a first electrode) and a second front-side conductor pattern **132** (e.g., a second electrode) are formed on the front side **112** of the piezoelectric layer **110**. A back-side conductor pattern **134** (e.g., a floating electrode) is formed on the second side **114** of the piezoelectric layer **110**. The back-side conductor pattern **134** is a "floating" conductor pattern, meaning that is not electrically connected to any other conductor. Moreover, the back-side conductor pattern **134** is capacitively coupled to the first and second front-side conductor patterns **130**, **132**. The conductor patterns may be molybdenum, aluminum, copper, gold, or some other conductive metal or alloy. The back-side conductor pattern and the front side conductor patterns are not necessarily the same material. In an exemplary aspect, the back-side conductor pattern **134** can be made of any appropriate electrically conductive material. For example, the back-side electrode may be gold to avoid corrosion. The portion of the piezoelectric layer **110** between the first front-side conductor pattern **130** and the back-side conductor pattern **134** forms a first resonator **150**. The portion of the piezoelectric layer **110** between the second front-side conductor pattern **132** and the back-side conductor pattern **134** forms a second resonator **155**. The first and second resonators **150**, **155** are electrically in series such that an RF signal applied between the first and second front-side conductor patterns **130**, **132** excites acoustic waves in both the first and second resonators **150**, **155**.

[0055] According to an exemplary aspect, the diaphragm forms a seal over the cavity **125** such that the first and second front-side conductor patterns **130**, **134** are not exposed to the environment adjacent to the back-side conductor pattern **134**. Ideally, when an RF signal is applied between the first and second front-side conductor patterns **130**, **132**, the back-side conductor pattern should remain at ground potential. To this end, a capacitance of the first resonator **150** should be equal to a capacitance of the second resonator **155**. Assuming the piezoelectric diaphragm has uniform thickness, the capacitances will be equal if the area of the first resonator **150**, which is to say the area of overlap between the first front-side conductor pattern **130** and the back-side conductor pattern **134**, is equal to the area of the second resonator **155** which is the area of overlap between the second front-side conductor pattern **132** and the back-side conductor pattern **134**. The back-side conductor pattern **134** will remain at ground potential when balanced signals (i.e., signals with equal amplitude and 180-degree phase difference), are applied to the first and second conductor patterns **130**, **132**. Moreover, one or more additional layers **140** can be disposed on the back-side conductor pattern **134** that is opposite the piezoelectric layer **110**. The one or more additional layers **140** can be a dielectric layer, a sensor layer or the like, that can convert the resonator to a sensor in an exemplary aspect. For example, a sensing layer **140** may be provided, for example, as a film, a monolayer, or a surface treatment that is either disposed directly on the back-side conductor pattern **134** or may be coupled to the back-side conductor pattern **134** via one or more additional an intermediate layers, such as an adhesion layer.

[0056] According to the exemplary aspect, the piezoelectric layer **110** may be Y-cut (i.e., with the Y crystalline axis of the piezoelectric material normal to the surfaces **112**, **114**) or rotated Y-cut (i.e., with the Y crystalline axis of the piezoelectric material rotated by a predetermined angle with respect to normal to the surfaces **112**, **114**). In this case, an RF signal applied between the first and second front-side conductor patterns **130**, **132** will excite shear acoustic waves in both the first and second resonators **150** and **155**. Rotated Y-cuts can be used to achieve shear displacements exclusively in planes parallel to the surface **112**, **114**. Selection of the rotation angle can be used to control the electromechanical coupling of the resonators. Shear displacements parallel to the surfaces of the piezoelectric layer do not generate compressional waves in an adjacent liquid thus allowing high Q-factor operation of the resonator.

[0057] As shown in FIG. **1**, the first and second front-side conductor patterns **130** and **132** and the back-side conductor pattern **134** are rectangular in shape. However, the conductor patterns may be non-rectangular (e.g., trapezoidal, curved, or irregular) to suppress parasitic acoustic modes according to alternative aspects.

[0058] In the detailed cross-sectional view, the thickness of the piezoelectric layer **110** is dimension ts and the thickness of the conductor patterns **130**, **132**, **134** is dimension tm. The thickness ts of the piezoelectric layer **110** may be, for example, 100 nanometers (nm) to 1000 nm according to an exemplary aspect. Moreover, the thickness tm of the conductor patterns **130**, **132**, **134** may be, for example, 10 nm to 500 nm. The thickness of the conductor patterns may be the same or the first and second front-side conductor patterns **130** and **132** and the back-side conductor pattern **134** may have different thicknesses from each other in an exemplary aspect.

[0059] As further shown, the piezoelectric layer may be etched or otherwise removed, completely or only partially, in the area between the first and second front-side conductor patterns **130**, **132**, forming slots **115**. The presence of the slots **115** may suppress lateral acoustic modes that might be excited by the electric field between the front-side conductor patterns **130**, **132**. A depth tg of the slot **115** can extend partially or completely through the piezoelectric layer **110**.

[0060] FIG. **2**A shows a simplified top view and a cross-sectional view of another YBAR **200**A. The YBAR **200**A is made up of a piezoelectric layer **210** attached to a substrate **220** as previously described. A cavity **225** (identified by dashed lines) is formed in the substrate **220** such that a portion of the piezoelectric layer **210** is suspended over the cavity **225**.

[0061] First and second front-side conductor patterns **230**, **232** (e.g., first and second electrodes) are formed on the front side of the piezoelectric layer (the side facing away from the cavity **225**). The first and second front-side conductor patterns **230**, **232** form an interleaved finger pattern (IFP) similar to an interdigital transducer or IDT used in surface acoustic wave resonators. The first front-side conductor pattern **230** includes a first plurality of parallel fingers extending (e.g., substantially parallel) from a first busbar. The second front-side conductor pattern **232** includes a second plurality of parallel fingers extending (e.g., substantially parallel) from a second busbar. The first and second pluralities of parallel fingers are interleaved and most or all

of the interleaved parallel fingers are disposed on the portion of the piezoelectric layer **210** that is over the cavity **225**. The width m of each finger will be a substantial portion of the pitch p, or center-to-center spacing, between at least a pair of interleaved fingers extending from different busbars.

[0062] As shown in the detail view, slots **215** may be formed in the piezoelectric layer **210** between the interleaved fingers of the first and second front-side conductor patterns **230**, **232** in an exemplary aspect. The presence of the slots **215** may suppress lateral acoustic modes that might be excited by the electric field between the front-side conductor patterns **230**, **232**. A depth tg of the slots **215** can extend partially or completely through the piezoelectric layer **210**. The grooves also prevent spreading of vibration energy along the structure thus improving Q-factor of resonators.

[0063] A back-side conductor pattern **234** is formed on the back side of the piezoelectric layer **210** opposed to the first and second front-side conductor patterns **230**, **232**. A first resonator is formed between the first front-side conductor pattern **230** and the backside conductor pattern **234**. A second resonator is formed between the second front-side conductor pattern **232** and the back-side conductor pattern **234**. The first and second front-side conductor patterns may have the same number of interleaved fingers in an exemplary aspect. Moreover, one or more additional layers **240** can be disposed on the back-side conductor pattern **234** that is opposite the piezoelectric layer **210**. The one or more additional layers **240** can be a dielectric layer, a sensor layer or the like to convert the resonator to a sensor in an exemplary aspect. For example, the sensing layer **240** may be, for example, a film, a monolayer, or a surface treatment that is either disposed directly on the back-side conductor pattern **234** or may be coupled to the back-side conductor pattern **234** via one or more additional an intermediate layers, such as an adhesion layer.

[0064] FIG. **2**B illustrates a schematic plan view and schematic cross-sectional views of a variation of the YBAR shown in FIG. **2**A according to another exemplary aspect. It is noted that the plan view of YBAR **200**B generally comprises the same elements of YBAR **200**A, which includes a piezoelectric layer **210** attached to a substrate **220**, and first and second front-side conductor patterns **230**, **232**, as previously described.

[0065] However, instead of having a cavity, YBAR **200**B includes an acoustic Bragg reflector **250** that is between (e.g., "sandwiched") the substrate **220** and the back surface of the piezoelectric plate **210**. The term "sandwiched" means the acoustic Bragg reflector **250** is both disposed between and physically connected to a surface of the substrate **220** and the back surface of the piezoelectric plate **210**. In some circumstances, thin layers of additional materials may be disposed between the acoustic Bragg reflector **250** and the surface of the substrate **220** and/or between the acoustic Bragg reflector **250** and the back surface of the piezoelectric plate **210**. Such additional material layers may be present, for example, to facilitate bonding the piezoelectric plate **210**, the acoustic Bragg reflector **250**, and the substrate **220**.

[0066] According to the exemplary aspect, the acoustic Bragg reflector **250** includes multiple layers that alternate between materials having high acoustic impedance and materials having low acoustic impedance. "High" and "low" are relative terms. For each layer, the standard for comparison is the adjacent layers. Each "high" acoustic impedance layer has an acoustic impedance higher than that of both the adjacent low acoustic impedance layers. Each "low" acoustic impedance layer has an acoustic impedance lower than that of both the adjacent high acoustic impedance layers. In an exemplary aspect, each of the layers can have a thickness equal to, or about, one-fourth of the acoustic wavelength at or near a resonance frequency of the SM XBAR **200**. Materials having comparatively low acoustic impedance include silicon dioxide, silicon oxycarbide, aluminum, titanium, and certain plastics such as cross-linked polyphenylene polymers. Materials having comparatively high acoustic impedance include silicon nitride, aluminum nitride, silicon carbide, and metals such as molybdenum, tungsten, gold, and platinum. All of the high acoustic impedance layers of the acoustic Bragg reflector **250** are not necessarily the same material, and all of the low acoustic impedance layers are not necessarily the same material.

[0067] An exemplary cross-sectional view is shown along the section plane C-C of YBAR **200**B. As shown, a space **215** (e.g., a cavity) is defined or formed in the first and second front-side conductor patterns **230**, **232** and the piezoelectric plate **210** to provide acoustic isolation between adjacent fingers. The space or cavity may be formed in the respective layers by etching or otherwise removed to effectively form slots as the cavity **215**. The presence of the cavity **215** suppresses lateral acoustic modes that might be excited by the electric field between the front-side conductor patterns **230**, **232**.

[0068] FIG. **3**A and FIG. **3**B show two exemplary cross-sectional views along the section plane B-B defined in FIG. **2**A of YBAR **200**A. It is noted that the configurations of the substrate **320** shown in FIGS. **3**A and **3**B may also be implemented for the YBAR configuration shown in FIG. **1**. In FIG. **3**A, a piezoelectric layer **310**, which corresponds to piezoelectric layer **210**, is attached directly to a substrate **320**, which can correspond to substrate **220** of FIG. **2**A. Moreover, a cavity **340**, which does not fully penetrate the substrate **320**, is formed in the substrate under the portion (i.e., the diaphragm **315**) of the piezoelectric layer **310** containing the interleaved fingers of the IDT of an YBAR. The cavity **340** can correspond to cavity **225** of FIG. **2**A and/or the cavity **125** of FIG. **1**. In an exemplary aspect, the cavity **340** may be formed, for example, by etching the substrate **320** before attaching the piezoelectric layer **310**. Alternatively, the cavity **340** may be formed by etching the substrate **320** with a selective etchant that reaches the substrate through one or more openings provided in the piezoelectric layer **310**.

[0069] FIG. **3**B illustrates an alternative aspect in which the substrate **320** includes a base **322** and an intermediate layer **324** that is disposed between the piezoelectric layer **310** and the base **322**. The intermediate layer **324** may, for example, be a dielectric layer. The intermediate layer **324** may be comprised of one or multiple layers between the base **322** and the piezoelectric layer **310**. For example, the base **322** may be silicon (e.g., a silicon support substrate) and the intermediate layer **324** may be a silicon oxide or dioxide or silicon nitride or some other material, e.g., an intermediate dielectric layer. That is, in this aspect, the base **322** and the intermediate layer **324** are collectively considered the substrate **320**. As further shown, cavity **340** is formed in the intermediate layer **324** under the portion (i.e., the diaphragm **315**) of the piezoelectric layer **310** containing the IDT fingers of a YBAR. In some cases, the cavity may be entirely

disposed in the intermediate layer **324** with a portion of the intermediate layer **324** being attached to a portion (i.e., the diaphragm **315**) of the piezoelectric layer **310** over the cavity **340**. The cavity **340** may be formed, for example, by etching the intermediate layer **324** before attaching the piezoelectric layer **310**. Alternatively, the cavity **340** may be formed by etching the intermediate layer **324**. In other example embodiments, the cavity **340** may be defined in the intermediate layer **324** by other means from whether the intermediate layer **324** was etched to define the cavity **340**. In some cases, the etching may be performed with a selective etchant that reaches the substrate through one or more openings (not shown) provided in the piezoelectric layer **310**. A thin layer of dielectric (not shown) may also be on the underside of piezoelectric layer **310** that faces the intermediate layer **324** and encloses the cavity **340** in an exemplary aspect.

[0070] In this case, the diaphragm **315**, which can correspond to the diaphragm of either of FIG. **1** and/or FIG. **2**A, for example, may be contiguous with the rest of the piezoelectric layer **310** around a large portion of a perimeter of the cavity **340**. For example, the diaphragm **315** may be contiguous with the rest of the piezoelectric layer **310** around at least 50% of the perimeter of the cavity **340**. As shown in FIG. **3**B, the cavity **340** extends completely through the intermediate layer **324**. That is, the diaphragm **315** can have an outer edge that faces the piezoelectric layer **310** with at least 50% of the edge surface of the diaphragm **315** coupled to the edge of the piezoelectric layer **310** facing the diaphragm **315**. This configuration provides for increased mechanical stability of the resonator.

[0071] In other configurations, the cavity **340** may partially extend into, but not entirely through the intermediate layer **324** (i.e., the intermediate layer **324** may extend over the bottom of the cavity on top of the base **322**) or may extend through the intermediate layer **324** and into (either partially or wholly) the base **322**. As described above, it should be appreciated that the interleaved fingers of the IDT can be disposed on either or both surfaces of the diaphragm **315** in FIGS. **3**A and **3**B according to various exemplary aspects. It is also noted while the exemplary aspect contemplates the resonator structures utility a membrane-based resonator structure, the resonator structures can be solidly mounted on metallic Bragg stack (mirror or reflector) for improved reliability in an alternative aspect, for example, using a configuration as described above with respect to FIG. **2**B.

[0072] FIG. **4**A illustrates a schematic plan view and a perspective view of an acoustic resonator structure that is a refinement of the exemplary aspect of the YBAR shown in FIG. **2**A. It should be appreciated that the acoustic resonator structure shown in FIG. **4**A can also be configured to have an acoustic Bragg reflector configuration as described above with respect to the YBAR configuration of FIG. **2**B. The X and Y axes are shown relative to the plan view in FIG. **4**A. FIG. **4**B illustrates a cross-section view of the IDT configuration in FIG. **4**A. The Z axis in FIG. **4**B is orthogonal to the plane defined by the X and Y axes of FIG. **4**A.

[0073] As shown, the electrode fingers (e.g., a pair) extend from a pair of busbars in a similar configuration as described above. In an exemplary aspect, the plurality of electrode fingers (also referred to as nanowires) each extend from a busbar predominantly in a first direction (e.g., substantially parallel to each other). Each of the electrode fingers includes an electrode **436**A (e.g., a top or first electrode) with a first potential (e.g., a positive potential) extending from a first busbar **430** is on top (e.g., a first side) of the piezoelectric layer **410** and an electrode **436**B (e.g., a bottom or second electrode) with a second potential (e.g., a negative potential) extending from a second busbar **432** is on the bottom (e.g., a second side) of the piezoelectric layer/material such that the electrode **436**A on the top of the piezoelectric layer **410** at least partially overlaps the electrode **436**B on the bottom of the piezoelectric layer **410**. As should be readily appreciated, the top and bottom electrodes **436**A and **436**B having isolated piezoelectric between them, such that a cavity (e.g., an air gap or some sort of insulating material such as a dielectric) provides for increased isolation of each adjacent top and bottom electrode pair and an adjacent top and bottom electrode pair. The YBAR configuration described below with respect to FIG. **5** as well as the configuration having piston masses as shown in FIG. **8** can each have isolation between the respective electrode fingers as well.

[0074] It is noted that while the piezoelectric layer **410** is shown to have a same width in the X-direction as the first and second electrodes, the piezoelectric layer can have a larger width in the X direction in an alternative aspect, such that the electrodes have a smaller width than the piezoelectric layer (in the X-direction). The piezoelectric layer **410** can also have different cross-sectional shapes besides a rectangular shape, such as a hexagonal shape. Moreover, while the corners/edges of the piezoelectric layer **410** and the electrics are shown to have a 90 degree or right angle, it should be appreciated that these corners or edges can be rounded or curved in practice, which may result from the deposition and/or etching processes as would be appreciated to one skilled in the art. Yet further, it should be appreciated that the electrodes **436**A and/or **436**B could have a wider width (i.e., in the X-direction) than the piezoelectric layer **410** and that the top and bottom electrodes can also have different widths from one another. It should be appreciated that these configurations can be applied to each of the embodiments shown in FIGS. **4**A, **4**B, **5** and/or **8**, for example.

[0075] FIG. **4**B illustrates how the electrode **436**B with the second potential extends into a cavity of the acoustic resonator, for example, cavity **125**/**225**, as described above. This configuration is described as a McBAW resonator in an exemplary aspect. As noted above, the cavity can be disposed directly in the substrate as shown in FIG. **3**A. Alternatively, the cavity can be disposed in an intermediate layer (e.g., a dielectric layer) between the substrate and the IDT structure as shown in FIG. **3**B.

[0076] Thus, according to the exemplary aspect shown in FIGS. **4**A and **4**B, an acoustic resonator is provided that includes a substrate (e.g., a substrate **420** in FIG. **4**B); a piezoelectric layer (e.g., the piezoelectric layer **410**) coupled to the substrate either directly or via one or more intermediate layers; a first conductor pattern forming a plurality of first electrodes **436**A disposed on a first surface of the piezoelectric layer (which has a first potential); and a second conductor pattern forming a plurality of second electrodes **436**B disposed on a second surface of the piezoelectric layer **410** opposite the first surface (which has a second potential). In this aspect, the respective electrodes of the first and second conductor patterns with the piezoelectric layer disposed therebetween collectively form at least a pair of electrode fingers (also referred to as "acoustically resonant

nanowires") extending in a first direction from a busbar and acoustically isolated, or at least acoustically insulated, from each other by way of a cavity or space disposed between the adjacent nanowires (e.g., the electrode fingers).

[0077] Thus, in the exemplary aspect, each of the plurality of nanowires extend from a busbar in a first direction (e.g., the y axis direction shown in FIG. **4**A), such that a space is defined between the nanowires (e.g., at least a pair of nanowires of the plurality of nanowires) in a second direction (e.g., the x axis direction shown in FIG. **4**A) that is substantially perpendicular to the first direction. In this regard, there is no piezoelectric material between the pair of nanowires in the second direction. In other words, as further illustrated in FIG. **4**A, the conductor patterns and piezoelectric material may be removed in the x and y area between adjacent pairs of top and bottom electrodes such that the fingers (i.e., nanowires) formed by each top and bottom electrode pair are substantially acoustically isolated, or at least partially acoustically isolated from one another as the piezoelectric layer does not connect one finger to the next finger. Accordingly, the top and bottom electrodes having isolated piezoelectric between each top and bottom electrode can be isolated from an adjacent top and bottom electrodes having piezoelectric therebetween by a cavity (such as a space or an air gap), some sort of insulating material such as a dielectric, or any other arrangement that allows for increased isolation of each adjacent top and bottom electrode pair and an adjacent top and bottom electrode pair. An exemplary YBAR configurations having this acoustic isolation configuration is described above with respect to FIG. **2**B, for example.

[0078] As described in more detail below, the pair of electrode fingers each comprise a width in a second direction that is substantially perpendicular to the first direction and a height in a thickness direction that is substantially orthogonal to the first and second directions. The ratio of the width to the height of each electrode finger is less than 2 in order to reduce spurs during excitation of the resonator device. As further shown, the acoustic resonator includes a pair of busbars (similar to the configuration described above), where a first busbar of the pair of busbars is coupled to the first conductor pattern, and a second busbar of the pair of busbars is coupled to the second conductor pattern. It is noted that the term "substantially" (e.g., "substantially perpendicular" and/or "substantially orthogonal") means that the relative directions are generally perpendicular or orthogonal, but may vary slightly (e.g., by 10 degrees) to take into account minor tolerances for manufacturing variances.

[0079] FIG. **5** illustrates a schematic plan view and a perspective view of an IDT configuration of another refinement of the exemplary aspect of the YBAR shown in FIG. **2**A. It should be appreciated that the acoustic resonator structure shown in FIG. **5** can also be configured to have an acoustic Bragg reflector configuration as described above with respect to the YBAR configuration of FIG. **2**B. In either event, in the configuration of FIG. **5**, the two electrodes **536**A and **536**B with positive and negative potentials are both on a first side (e.g., top side or surface) of the piezoelectric layer **510** whereas a floating electrode **536**C is on the opposing (e.g., second) side (e.g., bottom side or surface) of the piezoelectric layer **510**. A similar configuration is described above with respect to FIG. **1**, except that this configuration includes a plurality (e.g., pair) of electrode fingers. The exemplary acoustic resonator structure shown in FIG. **5** is similar to that described above in FIGS. **4**A and **4**B, except that it provides for a YBAR configuration in which a first busbar **530** of the pair of busbars is coupled to the first conductor pattern (e.g., fingers **536**A), and a second busbar **532** of the pair of busbars is coupled to the second conductor pattern (e.g., fingers **536**B). Moreover, a floating conductor pattern is the floating electrode **536**C that at least partially overlaps conductor patterns **536**A and **536**B. It is noted that while the piezoelectric layer **510** is shown to have a same width in the X-direction as the first and second electrodes, the piezoelectric layer **510** can have a larger width in the X direction in an alternative aspect.

[0080] According to the exemplary aspects in FIGS. **4**A, **4**B and **5**, the acoustic resonators are configured such that an X-dimension of the fingers (i.e., the width in the X-direction) is reduced to a minimum to form a single pair of electrodes as shown therein. As a result, an array of electrode pairs can be arranged and since they are separated by vacuum, the electrode pairs are acoustically isolated, or at least partially acoustically isolated, from one another by way of space or a cavity between adjacent fingers since the piezoelectric material is limited to be between, or substantially between, the top and bottom electrodes. According to this configuration, when the X-dimension of the electrode fingers is reduced to a minimum, the physics become quasi-1D and the X-dependent spurs will occur only at high frequencies in operation.

[0081] FIG. **6** illustrates a top view of the IDT configuration in FIGS. **4**A and **4**B according to an exemplary aspect. FIGS. **7**A and **7**B illustrate graphs of an admittance [y] as a function of frequency of an acoustic resonator according to an exemplary aspect.

[0082] According to an exemplary aspect, the piezoelectric layer **410** may comprise lithium niobate having Euler angles of (90, 90, 30±4). This configuration provides for a very high electromechanical coupling (i.e., $k^2 \approx 0.39$), which is sufficient for Wi-Fi full-band without inductors. FIG. **7**A illustrates a two-dimensional (2D) simulation, which is simulated using finite element method (FEM) simulation techniques, for X-direction (2Dx) and illustrates admittance for an existing series resonator for WiFi-full band. It is also noted that the total area required by a resonator will depend on the etch process. FIG. **6** illustrates an estimation for the area required using 5 μm spacing between electrode pairs.

[0083] FIG. **7**B illustrates 2Dx FEM simulations with various linewidths according to an exemplary aspect. It is noted that the resonance frequency is insensitive to electrode width, meaning that the resonance broadening will not be detrimental compared with XBAR. However, the spurs are sensitive to the width and side-wall angle. For XBAR, the electrode dimensions should be fabricated precisely to control the impact of spurs. According to the exemplary aspects, if the linewidth is sufficiently narrow, all X-direction spurs will only occur at high frequency (e.g., greater than 9000 MHz). Moreover, the X-direction spurs will also be smoothed by normal variations of the electrode widths.

[0084] FIG. **8** illustrates a top view of another IDT configuration of the acoustic resonators shown FIGS. **4**A and **4**B according to an exemplary aspect. In this aspect, piston masses **460**A through **460**D are disposed on tops of the ends of the electrode fingers **436**A, respectively. The piston masses may be additional layers (e.g., metal) that are deposited adjacent the busbar **430** and on the free end of the

electrodes **436**A to address spurs. Thus, as shown, the acoustic resonator includes a pair of piston masses disposed on a top surface of the first conductor pattern forming the pair of electrode fingers. In an exemplary aspect, a first pair of piston masses **460**A and **460**B are disposed adjacent to a base (e.g., connection to busbar **430**) and a second pair of piston masses **460**C and **460**D on a free end of each of the pair of electrode fingers **436**A, respectively. The piston masses can generally be considered as an extra layer of metal, for example, that has a rectangular or square shape from a plan view thereof. Preferably, the piston masses **460**A-D have a same width (i.e., in the X-direction) as the first and second conductor patterns **436**A. The pairs of piston masses can be disposed on either the first conductor pattern and/or on both the first and second conductor patterns, such that they overlap each other in the plan view (i.e., the Z-direction).

[0085] FIGS. **9**A and **9**B illustrate graphs of an admittance [y] as a function of frequency of an acoustic resonator as shown in FIG. **8** according to an exemplary aspect. These graphs are also simulated using finite element method (FEM) simulation techniques. According to an exemplary aspect, there may be significant spurs in the aperture (i.e., the Y-direction). However, the piston masses **460**A-D are provided to suppress these spurs. FIG. **9**A illustrates a 2Dy compared to 2Dx simulation and the additional cavity modes. According to the exemplary aspect, these transverse modes are suppressed by the piston masses **460**A-D. FIG. **9**B illustrates an exemplary aspect of the piston mode, which illustrates the reduction in spurs.

[0086] FIG. **10** illustrates a cross-sectional view of an IDT finger (e.g., an acoustically resonant nanowire) of an acoustic resonator configuration as shown in either FIG. **4**A and/or FIG. **5** according to exemplary aspects. As should be appreciated, the exemplary electrode finger includes a first or top electrode **1032** and a second or bottom electrode **1034** with a piezoelectric layer **1010** disposed therebetween. According to the exemplary aspect, the width of at least one (or both) of the electrodes (e.g., denoted by width w in the X-direction) is less than two times the height in the thickness direction (e.g., denoted by height h in the Z-direction), where the height h is defined as the total height of the electrode fingers, i.e., the top electrode **1032**, the bottom electrode **1034**, and the piezoelectric layer **1010**. In some cases, the thickness direction may be orthogonal to either the top or bottom surface of the piezo. However, either the top or bottom surface of the piezo may have variances due to manufacturing tolerances in which case the thickness direction may be substantially orthogonal (as orthogonal as possible) to either the top or bottom surface of the piezo. In any case, the height h of the electrode finger may be measured from, and including, the bottom electrode to, and including, the top electrode. The non-limiting example shown in FIG. **10** illustrates the top electrode **1032** and bottom electrode **1034** each having a height of 96 nm and formed of aluminum. Moreover, the piezoelectric layer **1010** can be formed of lithium niobate and have a height of 354 nm.

[0087] Thus, according to the exemplary aspect, the ratio of x/z as shown in FIG. **10** is less than 2. Moreover, it is noted that the resonator performance is primarily set by the electrodes away from the piston masses (assuming they are included according to an exemplary aspect). As a result, it should be appreciated that if the aspect ratio x/z is less than 2, it will be smaller at the ends of the fingers where the piston masses are located (i.e., since the height increases). According to the exemplary aspect, the capacitance density is much higher than an XBAR structure due to a smaller active area. In addition, the thermal conductance is much higher due to metal that covers the top and bottom surfaces of the piezoelectric layer, so these effects may offset one another leaving the power-handling similar to XBAR.

[0088] FIG. **11**A illustrates a graph of an admittance [y] as a function of frequency of an acoustic resonator according to an exemplary aspect. FIG. **11**B illustrates a graph of the coupling coefficient k^2 as a function of an aspect ratio of an acoustic resonator according to an exemplary aspect. These graphs are also simulated using finite element method (FEM) simulation techniques.

[0089] According to the exemplary aspects, the aspect ratio (i.e., the width/total height of the electrode structure) should be minimized to avoid spurs. FIG. **11**A illustrates 2Dx FEM simulations with a fixed height and various widths. As shown, the acoustic resonator structures with smaller aspect ratio shift the X-direction spurs to higher frequencies. Thus, it should be appreciated that acoustic resonator structures according to the exemplary aspect with aspect ratios that are less than 1 are advantageous to minimize spurs. On the other hand, FIG. **11**B illustrates that for very small aspect ratios, the coupling decreases. Thus, according to the exemplary aspect, the acoustic resonator structure preferably has an aspect ratio that is less than 2.

[0090] FIG. **12**A illustrates a cross-sectional view of an IDT finger (e.g., an acoustically resonant nanowire) of an acoustic resonator configuration as shown in FIG. **8** according to an exemplary aspect. It is noted that the first cross-sectional view in the XZ plane that shown in FIG. **12**A generally corresponds to the configuration described above with respect to FIG. **10** and the details will not be repeated herein. Moreover, the second cross-sectional view in the ZY plane that shown in FIG. **12**A can correspond to the same configuration and includes the plurality of pistons as described above with respect to FIG. **8**. In this case, the piston can have an exemplary height of 120 nm.

[0091] FIGS. **12**B and **12**C illustrate graphs of an admittance [y] as a function of frequency of an acoustic resonator according to an exemplary aspect. As described above with respect to FIG. **8**, the transverse (i.e., the Y-direction) modes can be substantially and/or completely suppressed with piston masses. FIG. **12**B illustrates a 2Dy FEM simulation for the acoustic resonator structure without the piston masses, which illustrates the aperture-dependent transverse modes. The 2Dy FEM for the same acoustic resonator structure with piston masses added on top and bottom as described above with respect to FIG. **8** is also shown in which the transverse modes are shown to be completely suppressed. FIG. **12**C illustrates a simulation in full 3D FEM for the same acoustic resonator structure with piston masses, which also confirms the transverse mode suppression.

[0092] In yet another exemplary aspect, a multi-layer electrode may be used for vertical field excited resonators (e.g., YBAR, McBAW, ARN, and the like).

[0093] Specifically, FIGS. **13**A-**13**B depict stress field in laterally and vertically excited devices. In some examples, such as shown in FIG. **13**B, for a vertically excited structure **1302** such as ARN, YBAR, and McBAW, the electrodes lie along an acoustic path (e.g., Al) **1312**A-**1312**B, as indicated by stress field **1322**, significant acoustic energy/stress in the

metal can lead to significant acoustic loss in the electrodes. For a laterally excited device **1301**, such as an XBAR, shown in FIG. **13**A, the stress field **1321**, the metal doesn't lie along the acoustic path, the acoustic energy/stress is primarily confined to region between metal IDT (e.g., Al) **1311**, as such acoustic energy/stress in the metal is less and acoustic loss in the electrodes is minimal. To reduce (e.g., minimize) energy/acoustic damping in the electrode (e.g., the metal layer) for vertically excited structures, electrode materials with a higher Q factor may be used, the energy distribution within the electrode may be reduced (e.g., minimized), and an electrode thickness may be reduced.

[0094] According to an exemplary aspect of the disclosure, a multi-layer metal structure including multiple layers of electrodes along a thickness direction (e.g., the Z axis) may be used as a vertically excited structure. Examples of the vertically excited structure include an acoustic resonator structure such as shown in FIGS. **1**, **2**, **4**A-B, **5**, **8**, and the like.

[0095] FIG. **14** shows an example of a multi-layer metal structure (or a multi-layer electrode) for a first conductor pattern (TE) disposed on a first surface of the piezoelectric layer (Piezo) and for a second conductor pattern (BE) disposed on a second surface of the piezoelectric layer of an acoustic resonator structure according to an aspect of the disclosure. It should be appreciate that the structure shown in FIG. **14** can generally correspond to that shown in FIG. **13**B, except that the first conductor pattern (TE) may include a first electrode layer (TE1) having a first acoustic impedance (e.g., a high acoustic Z) and a second electrode layer (TE2) having a second acoustic impedance (e.g., a low acoustic Z) that is lower than the first acoustic impedance. The second conductor pattern (BE) may include a first electrode layer (BE1) having a first acoustic impedance (e.g., a high acoustic Z) and a second electrode layer (BE2) having a second acoustic impedance (e.g., a low acoustic Z) that is lower than the first acoustic impedance.

[0096] In an example, the multi-layer metal structure is symmetric, for example, a thickness (or a height) along the Z axis of TE1 is substantially identical to a thickness (or a height) along the Z axis of BE1. Similarly, a thickness (or a height) along the Z axis of TE2 is substantially identical to a thickness (or a height) along the Z axis of BE2. In addition, materials of TE1 and BE1 are substantially identical, and materials of TE2 and BE2 are substantially identical.

[0097] In some examples, the multi-layer metal structure is asymmetric.

[0098] In an example, such as shown in FIG. **14**, a number of the multiple layers of electrodes of the first conductor pattern is two, and a number of the multiple layers of electrodes of the second conductor pattern is two, and thus the multiple layers of electrodes is referred to as a 2-layer electrode or a 2-layer electrode structure.

[0099] In an example, such as shown in FIG. **14**, the first electrode layer (TE1) of the first conductor pattern is disposed between the second electrode layer (TE2) of the first conductor pattern and the piezoelectric layer (e.g., made from lithium niobate ($LiNbO_3$) or a similar synthetic salt formed from niobium, lithium, and oxygen), and the first electrode layer (BE1) of the second conductor pattern is disposed between the second electrode layer (BE2) of the second conductor pattern and the piezoelectric layer.

[0100] Referring to FIG. **14**, the 2-layer electrode where the thin high impedance metal TE1 or BE1 (e.g., tungsten (W), platinum (Pt), molybdenum (Mo), ruthenium (Ru), or the like) is placed closest to the piezoelectric layer (e.g., directly on the piezoelectric layer) followed by the low impedance metal (e.g., Al) TE2 or BE2 may be used, for example, to reduce (e.g., significantly reduce) energy and loss within the electrode layer(s) (e.g., TE and/or BE). Further, in some examples, benefits include a higher electromechanical coupling (e.g., a k2 improvement) and a reduction in trace resistance of the IDT. In contrast, a single-layer electrode using a high velocity material to reduce (e.g., minimize) energy and loss within the single-layer electrode is not as effective as the 2-layer electrode described in the disclosure. The high velocity material is described below with reference to FIGS. **18**A-**18**C. In some examples, the high velocity material refers to a material that is relatively stiff and has a relatively small density.

[0101] FIGS. **15**A-**15**C show displacements **1501**, **1502** and **1503**, stresses **1511**, **1512** and **1513**, and acoustic energies **1521**, **1522** and **1523** of three different electrode structures **1531**, **1532** and **1533**, respectively. The electrode structure **1531** is a 1-layer electrode including Al (e.g., both TE1 and TE2 are made of Al). The electrode structure **1532** is a 1-layer electrode including W. The electrode structure **1533** is a 2-layer electrode including W as TE1 and Al as TE2. FIGS. **15**A-**15**C show that using the 2-layer electrode structure **1533** where a thin high impedance metal (e.g., W, Pt, Mo, or the like) is placed closest to the piezoelectric layer followed by a low impedance metal (e.g., Al) can significantly reduce energy within the electrode structure **1533** (W and Al). Referring to FIGS. **15**A-**15**C, the distribution of the energy **1523** within the metal (Al and W) in FIG. **15**C is less than the distributions of the energies **1521** and **1522** within the metal (Al or W) of a single layer electrode in FIGS. **15**A and **15**B.

[0102] The multi-layer electrode structure such as the 2-layer electrode structure shown in FIG. **14** may be optimized, for example, by manipulating the geometry and/or the materials of the multi-layer electrode structure. In an aspect, the optimization may be determined using certain parameters (e.g., fd, Qm, k2, and/or the like) indicating performances of the multi-layer electrode structure. Manipulating the geometry of the multi-layer electrode structure may include controlling thicknesses of TE1, TE2, TE, BE1, BE2, BE, and/or the piezoelectric layer. In an aspect, the multi-layer electrode structure such as the 2-layer electrode structure shown in FIG. **14** may be optimized, for example, by controlling a ratio (indicated by h_{TE}/h_{piezo}) of a thickness of TE h_{TE} over a thickness of the piezoelectric layer h_{piezo}, a ratio (indicated by h_{TE1}/h_{TE}) of a thickness of TE1 h_{TE1} over the thickness of TE h_{TE}, a ratio (indicated by h_{BE}/h_{piezo}) of a thickness of BE h_{BE} over the thickness of the piezoelectric layer, a ratio (indicated by h_{BE1}/h_{BE}) of a thickness of BE1 h_{BE1} over the thickness of BE, and/or the like.

[0103] In an aspect, for the optimal electrode stack, parameters that characterize the acoustic resonator including a parameter fd, a quality factor (Qm), and an electromechanical coupling (k2) may be relatively large. An electrode stack (or a multi-layer electrode) may be optimized by determining the optimal ratio h_{TE}/h_{piezo} and the optimal ratio h_{TE1}/h_{TE} based on a parameter fd plot, a quality factor or Q-factor (Qm) plot, and/or an electromechanical coupling (k2) plot. In an example, fd is the frequency constant in m/s, that is the frequency times by the thickness of the piezoelectric layer h_{piezo}. In an example, Qm is a motional

Q-factor at resonance. In some examples, the 2-layer electrode are optimized to achieve relatively large fd, Qm, and/or k2.

[0104] FIGS. **16**A-**16**C show an fd plot, a Qm plot, and a k2 plot, respectively, for an acoustic resonator, such as an ARN, that has a 2-layer electrode structure shown in FIG. **14** according to an aspect of the disclosure. For the example shown in FIGS. **16**A-**16**C, layers TE1 and BE1 are formed with W, and layers TE2 and BE2 are formed with Al. Layer TE includes TEL and TE2 and layer BE includes BE1 and BE2. The piezoelectric layer (e.g., having Euler angles of (90, 90, 30) and made of $LiNbO_3$) is disposed between TE and BE. The quality factor Q_{piezo} of the piezoelectric layer is 5000. The quality factor Q_{metal} of the metal layer is 200. For each plot, the x-axis (the horizontal axis) indicates a ratio h_{TE}/h_{piezo} of the thickness of the electrode to the piezo thickness, and the y-axis (the vertical axis) indicates a ratio h_{TE1}/h_{TE} of the thickness of the first electrode layer W to the total thickness of the 2-layer electrode.

[0105] Referring to FIG. **16**B, a dashed line **1601** indicates that the 2-layer electrode is substantially identical to a single-layer electrode made of TE2 (which can be aluminum) since the ratio h_{TE1}/h_{TE} approaches 0. A dashed line **1602** indicates that the 2-layer electrode is substantially identical to a single-layer electrode made of TE1 (which is W) since the ratio h_{TE1}/h_{TE} approaches 1. A dashed line **1603**, within the dashed area **1605**, indicates that the 2-layer electrode is a composite electrode including the first electrode layer W and the second electrode layer Al since the ratio h_{TE1}/h_{TE} is between 0 and 1. The dashed area **1605** indicates a range of acceptable ratios of h_{TE1}/h_{TE} from roughly greater than 0.1 and less than 0.6. FIG. **16**B shows that the quality factor (Qm) increases when the ratio h_{TE1}/h_{TE} increases from 0 to an optimal ratio and when the ratio h_{TE1}/h_{TE} decreases from 1 to the optimal ratio, and thus using the 2-layer electrode may improve Qm. In the example shown in FIG. **16**B, the optimal ratio is in a range, such as between 0.2 to 0.5 (e.g., 0.3 to 0.4). FIGS. **16**A-**16**C show that a 2-layer electrode may improve Qm and k2 when compared with a single-layer electrode made of Al or W.

[0106] The range where the optimal ratio (e.g., the optimal ratio for h_{TE1}/h_{TE}) occurs may depend on which one or more parameters are used to optimize the ratio, e.g., whether the Qm is used (as shown in FIG. **16**B), whether the fd is used (as shown in FIG. **16**A), and/or whether the k2 is used (as shown in FIG. **16**C). In an example, the Qm is used (as shown in FIG. **16**B) to optimize the range where the optimal ratio (e.g., the optimal ratio for h_{TE1}/h_{TE}) occurs.

[0107] Referring to FIGS. **16**A-**16**B, when h_{TE1}/h_{TE} increases indicating using more of the first electrode layer, in an example, Qm increases and fd decreases. Thus, a trade-off may occur when optimizing the ratio for multiple parameters.

[0108] The range where the optimal ratio (e.g., the optimal ratio for h_{TE1}/h_{TE}) occurs may depend on the materials of the first electrode layer (TE1 and/or BE1) and/or the second electrode layer (TE2 and/or BE2), as shown in FIGS. **20**A-**20**C, FIGS. **21**A-**21**C, and FIGS. **22**A-**22**C.

[0109] In an aspect, the ratio h_{TE1}/h_{TE} of the height (or the thickness) of TE1 over the total thickness (or the total height) of the multiple layers of electrodes (TE) may be from 0.1 to 0.6. In an exemplary aspect, the ratio h_{BE1}/h_{BE} of the height (or the thickness) of BE1 over the total thickness (or the total height) of the multiple layers of electrodes (BE) may be from 0.1 to 0.6. In an aspect, the ratio h_{TE}/h_{piezo} of the total thickness of TE over the thickness of the piezoelectric layer may be from 0.1 to 0.5. In an aspect, the ratio h_{BE}/h_{piezo} of the total thickness of BE over the thickness of the piezoelectric layer may be from 0.1 to 0.5. The ratios may be determined based on graphs illustrating simulated results in FIGS. **20**A-**20**C, FIGS. **21**A-**21**C, and FIGS. **22**A-**22**C.

[0110] With a proper electrode ratio as described above, acoustic energy in the 2-layer metal (e.g., TE and/or BE) may be reduced (e.g., minimized) to reduce attenuation in lossy metal layers to improve the Q-factor and may increase coupling (e.g., a separation between the resonant frequency Fr and the anti-resonant frequency Fa). Moreover, in the exemplary aspect, TE and BE are made to be symmetric.

[0111] FIG. **17** shows simulated results of displacements ("D"), stresses ("S"), and energies ("E") of nine electrode structures, respectively. Each of the nine electrode structures has a 1-layer electrode. The three columns correspond to three different values (0.5, 1, and 2) of a stiffness ratio C_m/C_{LN}, C_m is the stiffness or elastic constant of the metal layer and C_{LN} is the stiffness or elastic constant of the piezoelectric layer. Accordingly, the electrode becomes stiffer from the left side to the right side. The three rows correspond to three different values (0.5, 1, and 2) of a density ratio ρ_m/ρ_{LN} of a density of the electrode ρ_m over a density of the piezoelectric layer ρ_{LN}. Accordingly, the electrode becomes heavier per unit volume from the top row to the bottom row.

[0112] FIG. **17** shows that energy (E) and therefore acoustic damping in the electrode may be reduced (e.g., minimized) by choosing a light (e.g., having a low ρ_m/ρ_{LN}) and stiff metal (e.g., having a high C_m/C_{LN}) which may be referred to as a high velocity metal that is located at a top-right corner in FIGS. **18**A to **18**C. In this example, the light and stiff metal (e.g., the high velocity metal) has a C_m/C_{LN} of 2 and a ρ_m/ρ_{LN} of 0.5.

[0113] FIGS. **18**A-**18**C show examples of optimal material parameters such as stiffness and density as indicated by C_m/C_{LN} and ρ_m/ρ_{LN}, respectively for the single electrode according to an aspect of the disclosure. The ratio h_{TE}/h_{piezo} is 0.2, and the ratio h_{BE}/h_{piezo} is 0.2 in the simulations used for FIGS. **18**A-**18**C. FIG. **18**A shows an fd plot indicating how the parameter fd varies with C_m/C_{LN} and ρ_m/ρ_{LN}. FIG. **18**B shows a Qm plot indicating how the parameter Qm varies with C_m/C_{LN} and ρ_m/ρ_{LN}. FIG. **18**B shows that a higher Qm (e.g., a maximal Qm) may be obtained by using a metal (e.g., the high velocity metal) with a high stiffness and a small density, which is also shown in FIG. **17**. FIG. **18**C shows a k2 plot indicating how the parameter k2 varies with C_m/C_{LN} and ρ_m/ρ_{LN}. FIG. **18**C shows that a higher k2 (e.g., a maximal k2) may be obtained by using a metal (e.g., also referred to as a high impedance metal) with a high stiffness and a high density, which is also shown at the bottom-right corner in FIG. **17** (with a C_m/C_{LN} of 2 and a ρ_m/ρ_{LN} of 2 in FIG. **17**).

[0114] Referring back to FIG. **17**, when C_m/C_{LN} is low (e.g., 0.5) and ρ_m/ρ_{LN} is high (e.g., 2), the metal may be referred to as a low velocity metal, and may result in a relatively large energy dissipation (e.g., the maximal energy) in the metal, which may not be optimal for many applications.

[0115] As described above, the 2-layer electrode may be optimized by manipulating the geometry of the 2-layer

electrode (e.g., described in FIGS. **16**A-**16**C) and by using different metal materials (e.g., described in FIGS. **17** and **18**A-**18**C) in the 1-layer electrode.

[0116] In an example, different metal materials are used for TE1 and BE1 in the 2-layer electrode. FIGS. **19**A-**19**C, **20**A-**20**C, and **21**A-**21**C show the effect of different metal materials as TE1 and BE1 in the 2-layer electrode.

[0117] FIGS. **19**A-**19**C show an fd plot, a Qm plot, and a k2 plot, respectively, for a vertically excited structure that has a 2-layer electrode structure shown in FIG. **14** according to an aspect of the disclosure. In the example shown in FIGS. **19**A-**19**C, TE1 and BE1 are formed with Ru, TE2 and BE2 are formed with Al. TE includes TE1 and TE2. BE includes BE1 and BE2. The piezoelectric layer is disposed between TE and BE with Euler angles [90°, 90°, 30°] and is made of lithium niobate (e.g., $LiNbO_3$). The quality factor Q_{piezo} of the piezoelectric layer is 5000. The quality factor Q_{metal} of the metal layer is 200. For each plot, the x-axis (the horizontal axis) indicates a ratio h_{TE}/h_{piezo} of the thickness of the electrode to the piezo thickness, and the y-axis (the vertical axis) indicates a ratio h_{TE1}/h_{TE} of the thickness of the first electrode layer Ru to the total thickness of the 2-layer electrode. FIGS. **19**A-**19**C show that a 2-layer electrode may improve Qm and k2 when compared with a single-layer electrode made of Ru or W.

[0118] FIGS. **20**A-**20**C show an fd plot, a Qm plot, and a k2 plot, respectively, for a vertically excited structure that has a 2-layer electrode structure shown in FIG. **14** according to an aspect of the disclosure. In the example shown in FIGS. **20**A-**20**C, TE1 and BE1 are formed with Pt, TE2 and BE2 are formed with Al. TE includes TE1 and TE2. BE includes BE1 and BE2. The piezoelectric layer is disposed between TE and BE with Euler angles [90°, 90°, 30°] and is made of lithium niobate ($LiNbO_3$). The quality factor Q_{piezo} of the piezoelectric layer is 5000. The quality factor Q_{metal} of the metal layer is 200. For each plot, the x-axis (the horizontal axis) indicates a ratio h_{TE}/h_{piezo} of the thickness of the electrode to the piezo thickness, and the y-axis (the vertical axis) indicates a ratio h_{TE1}/h_{TE} of the thickness of the first electrode layer Pt to the total thickness of the 2-layer electrode. FIGS. **20**A-**20**C show that a 2-layer electrode may improve Qm and k2 when compared with a single-layer electrode made of Pt or W. In an example, the 2-layer electrode may be used in a McBAW resonator.

[0119] FIGS. **21**A-**21**C show an fd plot, a Qm plot, and a k2 plot, respectively, for a vertically excited structure that has a 2-layer electrode structure shown in FIG. **14** according to an aspect of the disclosure. In the example shown in FIGS. **21**A-**21**C, TE1 and BE1 are formed with Mo, TE2 and BE2 are formed with Al. TE includes TE1 and TE2. BE includes BE1 and BE2. The piezoelectric layer is disposed between TE and BE with Euler angles [90°, 90°, 30°] and is made of lithium niobate ($LiNbO_3$). The quality factor Q_{piezo} of the piezoelectric layer is 5000. The quality factor Q_{metal} of the metal layer is 200. For each plot, the x-axis (the horizontal axis) indicates a ratio h_{TE}/h_{piezo} of the thickness of the electrode to the piezo thickness, and the y-axis (the vertical axis) indicates a ratio h_{TE1}/h_{TE} of the thickness of the first electrode layer Mo to the total thickness of the 2-layer electrode.

[0120] Comparing FIGS. **16**B, **19**B, **20**B and **21**B, the optimal range for the ratios h_{TE}/h_{piezo} and h_{TE1}/h_{TE} may depend on the materials in the 2-layer electrode. FIG. **16**B indicates that to achieve a relatively large Qm when TE1 and BE1 include W, the optimal range for the ratio h_{TE1}/h_{TE} is approximately from 0.2 to 0.5 (e.g., from 0.3 to 0.4). FIG. **19**B indicates that to achieve a relatively large Qm when TE1 and BE1 include Ru, the optimal range for the ratio h_{TE1}/h_{TE} is approximately 0.3 to 0.6 (e.g., 0.4 to 0.6). FIGS. **20**B and **21**B indicate that to achieve a relatively large Qm when TE1 and BE1 include Pt or Mo, the optimal range for the ratio h_{TE1}/h_{TE} is approximately 0.1 to 0.3 (e.g., 0.18 to 0.25). As TE1 is changed from (i) W or Ru to (ii) Pt or Mo, the thickness of TE1 is to be reduced in order to obtain a larger Qm.

[0121] FIG. **22**A is a schematic block diagram of a bandpass filter using the acoustic resonator structure according to an exemplary aspect. The bandpass filter **2200** has a conventional ladder filter architecture including three series resonators **2210**A, **2210**B, and **2210**C and two shunt resonators **2220**A and **2220**B. The series resonators **2210**A, **2210**B, and **2210**C are connected in series between a first port and a second port (hence the term "series resonator"). In FIG. **22**A, the first and second ports are labeled "In" and "Out", respectively. However, the filter **2200** is bidirectional and either port may serve as the input or output of the filter. At least two shunt resonators, such as the shunt resonators **2220**A and **2220**B, are connected from nodes between series resonators to a ground connection. A filter may contain additional reactive components, such as inductors, not shown in FIG. **22**A. All the shunt resonators and series resonators are acoustic resonators in the exemplary aspect. The inclusion of three series and two shunt resonators is an example. A filter may have more or fewer than five total resonators, more or fewer than three series resonators, and more or fewer than two shunt resonators. Typically, all of the series resonators are connected in series between an input and an output of the filter. All of the shunt resonators are typically connected between ground and the input, the output, or a node between two series resonators.

[0122] In the exemplary filter **2200**, the series resonators **2210**A, **2210**B, and **2210**C and the shunt resonators **2220**A and **2220**B of the filter **2200** are formed on at least one, and in some cases a single, piezoelectric layer of piezoelectric material bonded to a silicon substrate (not visible). However, in alternative aspects, the individual resonators may each be formed on a separate piezoelectric layer bonded to a separate substrate, for example. Moreover, each resonator includes a respective IDT (not shown), with at least the fingers of the IDT disposed over a cavity, or an acoustic mirror, in the substrate. In this and similar contexts, the term "respective" means "relating things each to each," which is to say with a one-to-one correspondence. In FIG. **22**A, the cavities are illustrated schematically as the dashed rectangles (such as the rectangle **2235**). In this example, each IDT is disposed over a respective cavity. In other filters, the IDTs of two or more resonators may be disposed over a single cavity.

[0123] Each of the resonators in the filter **2200** has a resonance where the admittance of the resonator is very high and an anti-resonance where the admittance of the resonator is very low. The resonance and anti-resonance occur at a resonance frequency and an anti-resonance frequency, respectively, which may be the same or different for the various resonators in the filter **2200**. In simplified terms, each resonator can be considered a short-circuit at its resonance frequency and an open circuit at its anti-resonance frequency. The input-output transfer function will be near zero at the resonance frequencies of the shunt resonators and

at the anti-resonance frequencies of the series resonators. In a typical filter, the resonance frequencies of the shunt resonators are positioned below the lower edge of the filter's passband and the anti-resonance frequencies of the series resonators are positioned above the upper edge of the passband.

[0124] The frequency range between resonance and anti-resonance frequencies of a resonator corresponds to the coupling of the resonator. Depending on the design parameters of the filter **2200**, each of the resonators may have a particular coupling parameter to which the respective resonator is tuned in order to achieve the required frequency response of the filter **2200**. According to an exemplary aspect, each of the series resonators **2210**A, **2210**B, and **2210**C and the shunt resonators **2220**A and **2220**B can have an acoustic resonator configuration as described above with respect to FIGS. **1-2**, **4**A, **4**B, **5**, **6** and **8**.

[0125] FIG. **22**B is a schematic diagram of a radio frequency module that includes an acoustic wave filter of FIG. **22**A according to an exemplary aspect. In particular, FIG. **22**B illustrate a radio frequency module **2240** that includes one or more acoustic wave filters **2244** according to an exemplary aspect. The illustrated radio frequency module **2240** also includes radio frequency (RF) circuitry (or circuit) **2243**. In an exemplary aspect, the acoustic wave filters **2244** may include one or more of filter **2200**, as described above with respect to FIG. **22**A.

[0126] The acoustic wave filter **2244** shown in FIG. **22**B includes terminals **2245**A and **2245**B (e.g., first and second terminals). The terminals **2245**A and **2245**B can serve, for example, as an input contact and an output contact for the acoustic wave filter **2244**. Although two terminals are illustrated, any suitable number of terminals can be implemented for a particular application. The acoustic wave filter **2244** and the RF circuitry **2243** are on a package substrate **2246** (e.g., a common substrate) in FIG. **22**B. The package substrate **2246** can be a laminate substrate. The terminals **2245**A and **2245**B can be electrically connected to contacts **2247**A and **2247**B, respectively, on the package substrate **2246** by way of electrical connectors **2248**A and **2248**B, respectively. The electrical connectors **2248**A and **2248**B can be bumps or wire bonds, for example. In an exemplary aspect, the acoustic wave filter **2244** and the RF circuitry **2243** may be enclosed together within a common package, with or without using the package substrate **2246**.

[0127] The RF circuitry **2243** can include any suitable RF circuitry. For example, the RF circuitry can include one or more radio frequency amplifiers (e.g., one or more power amplifiers and/or one or more low noise amplifiers), one or more radio frequency switches, one or more additional RF filters, one or more RF couplers, one or more delay lines, one or more phase shifters, or any suitable combination thereof. The RF circuitry **2243** can be electrically connected to the one or more acoustic wave filters **2244**. The radio frequency module **2240** can include one or more packaging structures to, for example, provide protection and/or facilitate easier handling of the radio frequency module **2240**. Such a packaging structure can include an overmold structure formed over the package substrate **2246**. The overmold structure can encapsulate some or all of the components of the radio frequency module **2240**.

[0128] Throughout this description, the embodiments and examples shown should be considered as exemplars, rather than limitations on the apparatus and procedures disclosed or claimed. Although many of the examples presented herein involve specific combinations of method acts or system elements, it should be understood that those acts and those elements may be combined in other ways to accomplish the same objectives. With regard to flowcharts, additional and fewer steps may be taken, and the steps as shown may be combined or further refined to achieve the methods described herein. Acts, elements and features discussed only in connection with one embodiment are not intended to be excluded from a similar role in other embodiments.

[0129] As used herein, "plurality" means two or more. As used herein, a "set" of items may include one or more of such items. As used herein, whether in the written description or the claims, the terms "comprising", "including", "carrying", "having", "containing", "involving", and the like are to be understood to be open-ended, i.e., to mean including but not limited to. Only the transitional phrases "consisting of" and "consisting essentially of", respectively, are closed or semi-closed transitional phrases with respect to claims. Use of ordinal terms such as "first", "second", "third", etc., in the claims to modify a claim element does not by itself connote any priority, precedence, or order of one claim element over another or the temporal order in which acts of a method are performed, but are used merely as labels to distinguish one claim element having a certain name from another element having a same name (but for use of the ordinal term) to distinguish the claim elements. As used herein, "and/or" means that the listed items are alternatives, but the alternatives also include any combination of the listed items.

It is claimed:

1. An acoustic resonator comprising:

a plurality of nanowires that each include:

a piezoelectric layer having a first surface and a second surface;

a first electrode on the first surface of the piezoelectric layer; and

a second electrode on the second surface of the piezoelectric layer,

wherein the plurality of nanowires each extend from a first busbar predominantly in a first direction, such that a space is defined between a pair of nanowires of the plurality of nanowires in a second direction that is substantially perpendicular to the first direction, such that there is no piezoelectric material between the pair of nanowires in the second direction,

wherein the plurality of nanowires each comprise a height in a thickness direction that is substantially orthogonal to the first and second directions, and

wherein the plurality of nanowires each comprises a ratio of a width in the second direction of at least one of the first electrode and the second electrode to the height of the nanowire that is less than 2.

2. The acoustic resonator according to claim **1**, further comprising a pair of busbars that includes the first busbar that is coupled to the first electrode of each of the plurality of nanowires and a second busbar that is coupled to the second electrode of each of the plurality of nanowires.

3. The acoustic resonator according to claim **2**, wherein the second electrode of each of the plurality of nanowires is a floating electrode.

4. The acoustic resonator according to claim **1**, further comprising a pair of piston masses disposed a top surface of the first electrode of each of the plurality of nanowires.

5. The acoustic resonator according to claim 4, wherein the pair of piston masses are disposed adjacent to a base and on a free end of each of the plurality of nanowires.

6. The acoustic resonator according to claim 1, wherein the first electrode of each of the plurality of nanowires comprises multiple layers of electrodes in the thickness direction, and the multiple layers of electrodes of the first electrode include a first electrode layer having a first acoustic impedance and a second electrode layer having a second acoustic impedance that is lower than the first acoustic impedance.

7. The acoustic resonator according to claim 6, wherein the second electrode of each of the plurality of nanowires comprises multiple layers of electrodes in the thickness direction, and the multiple layers of electrodes of the second electrode include a first electrode layer having a first acoustic impedance and a second electrode layer having a second acoustic impedance that is lower than the first acoustic impedance of the first electrode layer of the second electrode.

8. The acoustic resonator according to claim 7, wherein a number of the multiple layers of electrodes of the first electrode is 2, and a number of the multiple layers of electrodes of the second electrode is 2.

9. The acoustic resonator according to claim 7, wherein the first electrode layer of the first electrode is disposed between the second electrode layer of the first electrode and the piezoelectric layer, and the first electrode layer of the second electrode is disposed between the second electrode layer of the second electrode and the piezoelectric layer.

10. The acoustic resonator according to claim 6, wherein a ratio of a thickness of the first electrode layer of the first electrode to a thickness of the multiple layers of electrodes of the first electrode is between 0.1 to 0.6.

11. The acoustic resonator according to claim 7, wherein a ratio of a thickness of the first electrode layer of the second electrode to a thickness of the multiple layers of electrodes of the second electrode is between 0.1 to 0.6.

12. The acoustic resonator according to claim 6, wherein a ratio of a thickness of the multiple layers of electrodes of the first electrode to a thickness of the piezoelectric layer is between 0.1 to 0.5.

13. The acoustic resonator according to claim 7, wherein a ratio of a thickness of the multiple layers of electrodes of the second electrode to a thickness of the piezoelectric layer is between 0.1 to 0.5.

14. An acoustic resonator comprising:

a plurality of electrode fingers that each include:

a piezoelectric layer having a first surface and a second surface;

a top electrode on the first surface of the piezoelectric layer; and

a bottom electrode on the second surface of the piezoelectric layer,

wherein the top electrode of the plurality of electrode fingers each extend from a first busbar predominantly in a first direction, wherein a space is defined between a pair of electrode fingers in a second direction that is substantially perpendicular to the first direction such that there is no piezoelectric material between the pair of nanowires in the second direction,

wherein the plurality of electrode fingers each comprise a width in the second direction and a total height in a thickness direction that is substantially orthogonal to the first and second directions, and

wherein at least one finger of the plurality of electrode fingers comprises a ratio of the to the total height that is less than 2.

15. The acoustic resonator according to claim 14, wherein the width of the plurality of electrode fingers is defined as a width in the second direction of at least one of the first electrode and the second electrode of the respective at least one finger.

16. The acoustic resonator according to claim 14, wherein:

the first electrode of each of the plurality of electrode fingers comprises multiple layers of electrodes in the thickness direction, and the multiple layers of electrodes of the first electrode include a first electrode layer having a first acoustic impedance and a second electrode layer having a second acoustic impedance that is lower than the first acoustic impedance, and

the second electrode of each of the plurality of electrode fingers comprises multiple layers of electrodes in the thickness direction, and the multiple layers of electrodes of the second electrode include a first electrode layer having a first acoustic impedance and a second electrode layer having a second acoustic impedance that is lower than the first acoustic impedance of the first electrode layer of the second electrode.

17. The acoustic resonator according to claim 16, wherein the first electrode layer of the first electrode is disposed between the second electrode layer of the first electrode and the piezoelectric layer, and the first electrode layer of the second electrode is disposed between the second electrode layer of the second electrode and the piezoelectric layer.

18. The acoustic resonator according to claim 17, wherein:

a ratio of a thickness of the first electrode layer of the first electrode to a thickness of the multiple layers of electrodes of the first electrode is between 0.1 to 0.6, and

a ratio of a thickness of the first electrode layer of the second electrode to a thickness of the multiple layers of electrodes of the second electrode is between 0.1 to 0.6.

19. The acoustic resonator according to claim 17, wherein:

a ratio of a thickness of the multiple layers of electrodes of the first electrode to a thickness of the piezoelectric layer is between 0.1 to 0.5, and

a ratio of a thickness of the multiple layers of electrodes of the second electrode to a thickness of the piezoelectric layer is between 0.1 to 0.5.

20. A bandpass filter comprising:

a plurality of acoustic resonators comprising one or more series resonators and one or more shunt resonators, at least one acoustic resonator of the plurality of acoustic resonators including:

a plurality of nanowires that each include:

a piezoelectric layer having a first surface and a second surface;

a first electrode on the first surface of the piezoelectric layer; and

a second electrode on the second surface of the piezoelectric layer,

wherein the plurality of nanowires each extend from a first busbar predominantly in a first direction, such

that a space is defined between a pair of nanowires of the plurality of nanowires in a second direction that is substantially perpendicular to the first direction, such that there is no piezoelectric material between the pair of nanowires in the second direction,

wherein the nanowires each comprise a height in a thickness direction that is substantially orthogonal to the first and second directions, and

wherein the plurality of nanowires each comprises a ratio of a width in the second direction of at least one of the first electrode and the second electrode to the height of the nanowire that is less than 2.

* * * * *